

University of Vermont

**UVM ScholarWorks**

---

UVM Honors College Senior Theses

Undergraduate Theses

---

2014

## Small Unmanned Aerial Systems (sUAS) for Volume Estimation

Adam Zylka

*University of Vermont*

Follow this and additional works at: <https://scholarworks.uvm.edu/hcoltheses>

---

### Recommended Citation

Zylka, Adam, "Small Unmanned Aerial Systems (sUAS) for Volume Estimation" (2014). *UVM Honors College Senior Theses*. 44.

<https://scholarworks.uvm.edu/hcoltheses/44>

This Honors College Thesis is brought to you for free and open access by the Undergraduate Theses at UVM ScholarWorks. It has been accepted for inclusion in UVM Honors College Senior Theses by an authorized administrator of UVM ScholarWorks. For more information, please contact [scholarworks@uvm.edu](mailto:scholarworks@uvm.edu).

*Honors College Undergraduate Thesis*

# **Small Unmanned Aerial Systems (sUAS) for Volume Estimation**



The University of Vermont  
College of Engineering and Mathematical Sciences  
*Department of Civil and Environmental Engineering*

Adam Zylka

## **Faculty Advisors**

Dr. Donna Rizzo, Jarlath O'Neil-Dunne, Dr. Arne Bomblies

29 April, 2014

## Abstract

A crucial step in responding to destruction by natural disasters is to estimate the amount of material needed to rebuild and repair damaged infrastructure. Current practices may be time-consuming, expensive, and inaccurate. However, stereo imagery obtained from a small Unmanned Aerial System (sUAS) can be used to estimate volumes in a safe, inexpensive, and accurate manner. Generation of 3D point clouds and digital surface models from imagery collected by a SenseFly eBee sUAS yields data that are on par with terrestrial LiDAR sensors in terms of volume estimations, while the lightweight platform of a UAS allows for rapid and repeated deployment in the immediate aftermath of a major disaster event. These characteristics, in conjunction with the capability of this platform for the remote surveying of dangerous areas, could facilitate response to a disaster in less time and with increased accuracy and precision.

**DISCLAIMER:** The views, opinions, findings and conclusions reflected in this presentation are the responsibility of the authors only and do not represent the official policy or position of the USDOT/RITA, or any State or other entity.

# Table of Contents

Abstract .....	i
List of Figures .....	iii
List of Tables .....	iii
Introduction.....	1
Background.....	1
Literature Review.....	2
Materials .....	4
RIEGL VZ1000 Terrestrial Laser Scanner.....	4
SenseFly eBee sUAS .....	5
Data Collection .....	7
Study Site 1: Stockpile (Morrisville, VT).....	7
Terrestrial LiDAR.....	7
sUAS.....	7
Study Site 2: Manure Pit (Shelburne, VT).....	12
Terrestrial LiDAR.....	12
sUAS.....	12
Data Processing.....	16
Terrestrial LiDAR.....	16
sUAS.....	19
Volume Calculations.....	21
sUAS.....	23
Terrestrial LiDAR.....	28
Results.....	33
Stockpile Volume.....	33
Manure Pit Volume.....	34
Conclusions.....	35
Acknowledgements.....	37
Literature Review.....	37
Appendix A: Stockpile Volume Data .....	38
Appendix B: Manure Pit Volume Data.....	40
Appendix D: Morrisville sUAS Flight Quality Report.....	42
Appendix E: Shelburne sUAS Flight Quality Report.....	47
Appendix F: Standard Operating Guidelines .....	52

## List of Figures

Figure 1: RIEGL VZ1000 Terrestrial Laser Scanner and control point .....	4
Figure 2: SenseFly eBee sUAS.....	5
Figure 3: SenseFly eBee launch procedure.....	6
Figure 4: Location of stockpile in relation to Morrisville, VT .....	8
Figure 5: GCP locations in relation to stockpile.....	9
Figure 6: sUAS flight lines for stockpile mission.....	10
Figure 7: Overlap of sUAS imagery for stockpile mission.....	11
Figure 8: Location of manure pit in relation to Shelburne, VT .....	13
Figure 9: sUAS flight lines for manure pit mission.....	14
Figure 10: Overlap of sUAS imagery for manure pit mission.....	15
Figure 11: Terrestrial LiDAR point cloud and interpolated DSM (stockpile).....	17
Figure 12: Terrestrial LiDAR point cloud and interpolated DSM (manure pit).....	18
Figure 13: PostFlight Terra GCP Editor .....	20
Figure 14: Volume calculation process diagram .....	21
Figure 15: Cross section of minimum reference method.....	22
Figure 16: Cross section of cut reference method .....	22
Figure 17: Superposition of 30 unique stockpile base polygons (sUAS).....	24
Figure 18: Superposition of 30 unique manure pit base polygons (sUAS) .....	25
Figure 19: Interpolation of stockpile cut reference plane (sUAS).....	26
Figure 20: Interpolation of manure pit cut reference plane (sUAS).....	27
Figure 21: Superposition of 30 unique stockpile base polygons (terrestrial LiDAR) .....	29
Figure 22: Superposition of 30 unique manure pit base polygons (terrestrial LiDAR).....	30
Figure 23: Interpolation of stockpile cut reference plane (terrestrial LiDAR) .....	31
Figure 24: Interpolation of manure pit cut reference plane (terrestrial LiDAR) .....	32

## List of Tables

Table 1: Coordinates of GCPs (NAD83 VT State Plane).....	7
Table 2: Properties of Morrisville stockpile sUAS flight .....	9
Table 3: Properties of Shelburne sUAS Flight .....	12
Table 4: Interpolation settings for terrestrial LiDAR point clouds.....	16
Table 5: Results of stockpile volume calculations.....	34
Table 6: Results of manure pit volume calculations.....	35
Table 7: sUAS stockpile volumes.....	38
Table 8: LiDAR stockpile volumes .....	39
Table 9: sUAS manure pit volumes .....	40
Table 10: LiDAR manure pit volumes.....	41

## **Introduction**

Natural disasters can have profound impacts on the transportation networks of our nation. Accurate information about the location and extent of damage is critical for coordinating both short- and long-term recovery efforts. This demand is especially high in rural areas, where communication networks are often more vulnerable. In the case of Tropical Storm Irene, which passed over Vermont on August 28, 2011, an estimated 260 roads were made impassable and all east-west road systems in the southern portion of the state were closed. The majority of state government offices were flooded and key telecommunications infrastructure was damaged, which created a considerable challenge for the Vermont Agency of Transportation (VTTrans) in locating and repairing the damaged infrastructure.

Crucial data needed for the recovery process are estimates of the volume of fill required to repair the damage. Current practices for determining this amount of material are to perform a basic field survey or to simply estimate. In the rare situation where an entire roadway is destroyed, a full survey may be necessary. However, surveys can be arduous and could require weeks to collect and analyze the data to determine the fill requirements. During Irene, these methods of field surveying were found to be both slow and dangerous due to the periodic flash floods in the wake of the storm. Basic surveys and “eyeballing” by field engineers are quicker processes, but rely on cursory data, instinct, and general rule of thumb. Without complete knowledge about the extent of the damage, engineers must err on the side of caution regarding fill estimates. This inaccuracy can result in excess orders of fill, unnecessarily increasing the total cost of the recovery effort. Roadways consist of multiple layers of different fills with different prices, so a reliable estimate of the amounts of each needed is critical for an efficient and cost-effective recovery effort.

## **Background**

The use of small Unmanned Aerial Systems (sUAS) may offer some solutions to the challenges encountered during disaster response and recovery efforts. In conjunction with recent advances in miniaturizing mapping technologies, these autonomous self-propelled aircraft have the potential to provide a wide range of remote sensing opportunities. While this technology was previously available only for military applications, the introduction of low-cost commercial sUAS is beneficial for conducting operations that are too dangerous, time-consuming, or uneconomical to be carried out by

alternative methods. UAS have a number of advantages over piloted aircraft, including lower image acquisition costs, the capability to deploy quickly and repeatedly, and the ability to fly at low altitudes.

Small, light-weight UAS can be equipped with a variety of sensing equipment to record video or still images. Beyond the direct applications of these types of data, stereo-imagery can be utilized to generate three-dimensional (3D) point clouds. Programming a sUAS to follow an overlapping flight path results in imagery obtained from different angles. This data can be combined into a 3D point cloud through multi-view stereopsis (MVS) techniques and distributed as a digital surface model (DSM). The accuracy of this procedure is heavily dependent on the resolution of the obtained imagery and the capability of the processing software used (Neitzel & Klonowski, 2011). Commercial GIS software can be used to visualize these 3D models and calculate the volume of an area of interest. This study compares volume estimations from sUAS generated surface models to estimates obtained from models created by a highly accurate ground-based Light Detection and Ranging (LiDAR) sensor. The accuracy of volume estimates are assessed for two features: a stockpile of fill material and a manure pit. Validation of this process could allow recovery agencies to survey damage to infrastructure with more immediacy and precision.

## **Literature Review**

Though still maturing, UAS technology has already been able to fulfill the needs of response crews to identify and estimate the extent of damage after a number of natural disasters. In 2011, the combination of an earthquake and a tsunami devastated a nuclear reactor complex in Fukushima, Japan. Due to radiation danger, nuclear engineers and technicians from the Tokyo Electric Power Company (TEPCO) were not able to place sensors or physically enter the reactor sites themselves. This resulted in a gap in information about the severity and extent of the damage. A UAS was deployed from outside the danger zone and was able to relay still imagery and video clips to the response personnel (Madrigal, 2011). The data collected by this platform was critical in creating and updating the plan for repairing the extensive damage to the reactors.

UAS have also been deployed for post-disaster imagery collection after other earthquakes across the globe. Following an earthquake in L'Aquila, Italy in 2009, quad-copter UAS were deployed to evaluate their potential applications for fire service response (Murphy, 2011). After the devastating 2010 earthquake in Haiti, a private company flew a sUAS to assess damage to orphanages in the remote mountains outside Port-Au-Prince. Real-time imagery relayed by the UAS indicated that the critical

infrastructure of the orphanages remained intact, which allowed recovery efforts to be concentrated in other locations (Adams, 2011). A United States Air Force Global Hawk UAS also conducted missions to Haiti to inspect the damage to roads and airports. The extensive range and endurance of the Global Hawk, with the ability to fly daily missions between Maryland and Haiti, was of great value to the operation due to the lack of sufficient infrastructure near or in Haiti. During these 14 hour missions, over 700 high-resolution images were collected (Petcoff, 2010).

Due to their small size and low weight, commercial sUAS can also face a number of physical limitations to operation in post-disaster scenarios. Wind speed is an important factor regarding UAS capability. Strong winds can increase deviation from the proposed flight path and have negative repercussions for take-off and landing procedures. It is necessary to ensure proper atmospheric conditions are met before initiating a flight because non-ideal conditions could mitigate the potential time- and cost-saving advantages of a sUAS. This technology can also be fairly fragile and susceptible to damage upon landings in improper conditions, which would be likely to increase the cost of a project.

In the United States, there are bureaucratic limitations imposed by the Federal Aviation Administration (FAA), which initially authorized use of unmanned aircraft within the National Airspace System (NAS) in 1990. Currently, the FAA requires a Certificate of Authorization (COA) for public entities wishing to operate a UAS in civil airspace. A COA regulates the area of operation in accordance with visual flight rules, and puts limits on distance and altitude. To comply with the level of safety required by the FAA in terms of collision avoidance, observers or a chase plane must maintain visual contact with the UAS, as this technology cannot yet meet the “see and avoid” rules that apply to all conventional manned aircraft (Laliberte, 2010). This requirement for visual observers and specially trained personnel by a COA can add to the cost of an operation and the application process for the certificate can hinder deployment of drones in urgent situations, especially for disaster response. Looking to the future, the FAA’s newly established Unmanned Aircraft Systems Integration Office should be able to streamline the COA process to decrease application times, separate UAS by size, and allow the possibility of using the autonomous capability of these aircraft to access more remote locations (FAA, 2013). This will have a significant role in increasing potential applications in the United States for sUAS technology.



## Materials

### RIEGL VZ1000 Terrestrial Laser Scanner

Calibration data were collected with a RIEGL VZ1000 Terrestrial Laser Scanner provided by the University of Vermont College of Engineering and Mathematical Sciences. This device, pictured in Figure 1, is capable of taking high resolution and accurate 3D measurements using LiDAR technology. Each return from the laser pulse system has range and intensity values, as well as spatial location measured in three dimensions. When plotted in 3D space, these returns are referred to as a point cloud. By distributing reflective control targets around an area of interest, it is possible to combine the data collected by several scans at unique locations into a single composite point cloud. A control target can be seen in the upper left portion of Figure 1. This device was operated by Dr. Jeff Frolik and Hanna Anderson, an undergraduate Environmental Engineer at the University of Vermont.



*Figure 1: RIEGL VZ1000 Terrestrial Laser Scanner and control point*

## SenseFly eBee sUAS

The sUAS used in this assessment was a SenseFly eBee, which is currently under ownership of the US Department of Transportation (DOT) for use in a research project entitled “Rapid Exploitation of Commercial Remotely Sensed Imagery for Disaster Response & Recovery.” Use of this equipment was facilitated by the University of Vermont Spatial Analysis Laboratory (SAL) and the Transportation Research Center (TRC).

The eBee, shown in Figure 2, is a lightweight autonomous foam aircraft that contains an integrated 16 MP camera capable of recording aerial imagery at resolutions as fine as 2 cm/pixel. The entirety of this system’s hardware can be easily transported in a flight case and rapidly assembled in the field. With a well-practiced team following a set of established standard guidelines, the eBee can be deployed in a matter of minutes. A field-swappable rechargeable battery provides up to 45 minutes of flight time and allows the eBee to cover areas up to 10 km<sup>2</sup> (3.9 mi<sup>2</sup>) in a single flight. The system can be used in light rain or snow and can tolerate winds as high as 10 m/s (22 mph).



*Figure 2: SenseFly eBee sUAS*

Flight planning functionality and in-flight controls for eBee are accomplished using a laptop or tablet running SenseFly's eMotion2 software package. Flight patterns can be created prior to deployment in a safe and comfortable location, such as an office, or generated on the fly in the field. This flexibility could prove crucial by providing the ability to adjust to rapidly changing conditions in a post-disaster scenario. An integrated GPS unit and radio module facilitates communication between the eBee and the software to provide real-time flight monitoring. Notifications of in-flight warnings are displayed in the software. Through this interface, the eBee's mission can be aborted if necessary or, if the landing zone is not clear, the sUAS can be put into a circular holding pattern. Refer to the Standard Operating Guidelines attached as Appendix F for an in-depth tutorial on mission planning.

The simplicity of the eBee's launching and landing procedures could allow for rapid and repeated deployment following a disaster event. The launching procedure is demonstrated in Figure 3. The operator shakes the eBee three times to engage the motor. Once the motor reaches full power, the operator takes two steps forward and releases the eBee at a ten degree angle above the ground. The aircraft climbs steeply and circles around a user-specified waypoint to gain altitude before starting its preprogrammed mission. When the mission is complete and the landing procedure has been initiated by the flight operator, the eBee circles above the specified landing area to measure wind conditions. Once the direction and velocity of the wind is determined, the system calculates the ideal linear approach within an approach sector defined by the operator. The eBee decreases in altitude as it flies along this vector. As the system nears the landing zone, its optical sensor determines the location of the ground surface. When the aircraft is a few meters above the ground, the motor reverses abruptly in order to reduce velocity and then powers down. The eBee glides to the ground where it can be collected and prepared for its next mission.



*Figure 3: SenseFly eBee launch procedure*

## Data Collection

### Study Site 1: Stockpile (Morrisville, VT)

sUAS and terrestrial LiDAR data were collected for a stockpile on November 21, 2013. This pile was located at the construction site for the VTrans Morrisville Alternative Truck Route project in Morrisville, VT. The location of the pile relative to Morrisville is shown in Figure 4. An initial sUAS survey of the 3km construction corridor was conducted on November 20, 2013, during which the stockpile was identified as an ideal feature to use in this assessment.

#### *Terrestrial LiDAR*

Five unique scans were conducted around the perimeter of the stockpile with the RIEGL VZ1000 in order to create a composite point cloud that represented the entire feature. Ten reflective targets were placed around the vicinity of the stockpile to act as control points. Due to the height of the stockpile and limitations of the scanner, no returns were collected along the top surface of the pile, although reference was provided by a control target placed on top of this surface. The total on-site time from set-up to take-down for this data collection was approximately 4 hours.

#### *sUAS*

Prior to the flight, four ground control points (GCPs) were established around the extent of the area of interest. The use of GCPs ensures vertical and horizontal accuracy in the processed sUAS dataset. Each GCP was created by folding two white trash bags to a width of 2-3 inches and laying them across each other to form a cross. The GCPs were secured with small rocks and a Trimble Pathfinder ProXH receiver with Trimble Zephyr antenna was used to record their coordinate locations in the NAD 1983 Vermont State Plane datum. GCP locations are tabulated in Table 1 and displayed spatially in Figure 5. The inlay in the bottom left corner of this image shows a picture of one of the GCPs as set up in the field.

*Table 1: Coordinates of GCPs (NAD83 VT State Plane)*

<b>GCP</b>	<b>X (m)</b>	<b>Y (m)</b>	<b>Z (m)</b>
1	491718.777	229299.768	190.321
2	491742.907	229260.175	188.612
3	491722.086	229208.375	187.54
4	491693.816	229207.564	187.085



Figure 4: Location of stockpile in relation to Morrisville, VT

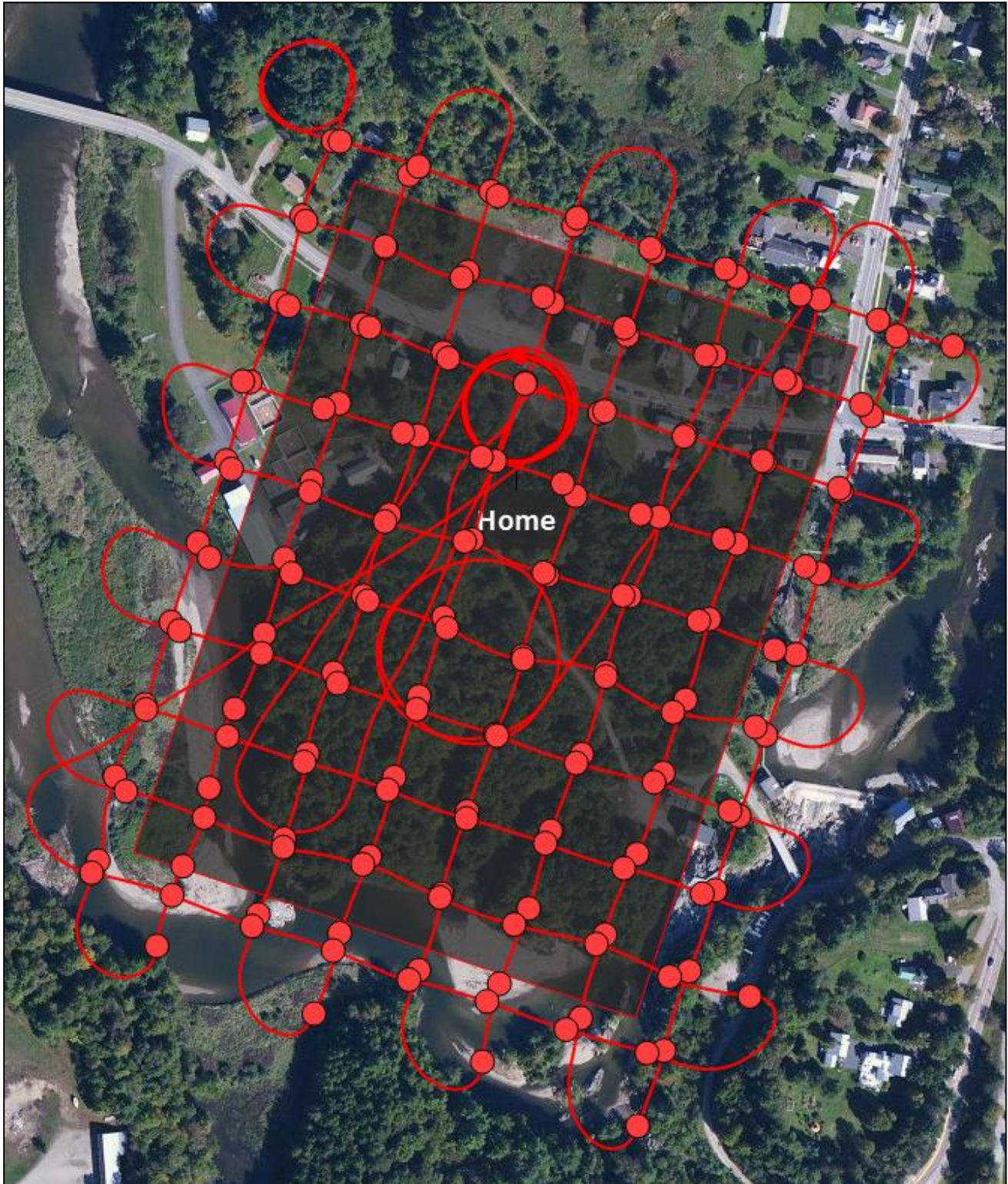


Figure 5: GCP locations in relation to stockpile

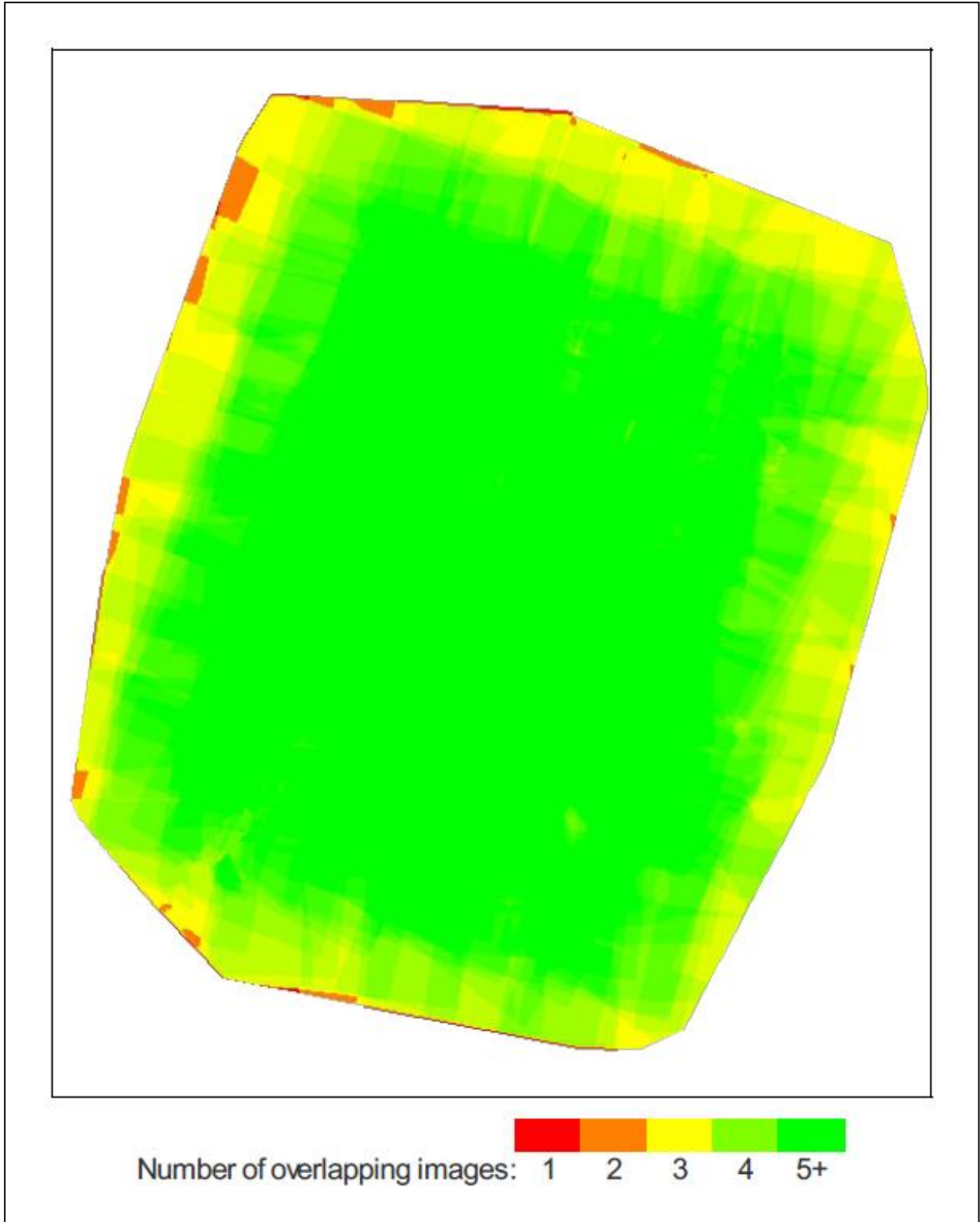
The properties of the eBee flight used in this analysis are presented in Table 2 and the flight path is displayed in Figure 6. Image count represents the total number of photographs taken by the eBee during the mission. The overlap of the collected imagery is displayed graphically in Figure 7. Image overlap is reduced significantly around the perimeter of the surveyed area. Ground resolution, measured in cm/pixel, is a function of the eBee's altitude above ground level (AGL). The surveyed mission area, as determined during post-processing, is tabulated in hectares. GCP error represents the difference between the measured location of the GCPs and their locations determined during data processing. The flight time for this area was approximately 30 minutes from take-off to landing.

Table 2: Properties of Morrisville stockpile sUAS flight

Image count	Resolution (cm/pixel)	Surveyed area (ha)	Total GCP error (cm)
166	3.25	12.01	1.3



*Figure 6: sUAS flight lines for stockpile mission*



*Figure 7: Overlap of sUAS imagery for stockpile mission*



## Study Site 2: Manure Pit (Shelburne, VT)

On December 3, 2013, sUAS and terrestrial LiDAR data were collected for a manure pit located on the grounds of Shelburne Farms in Shelburne, VT (Figure 8). This feature is somewhat analogous to a damaged roadway because it represents a void volume.

### *Terrestrial LiDAR*

Three scans were conducted at unique locations around the perimeter of the manure pit with the RIEGL VZ1000. Ten reflective targets were scattered throughout the area to ensure that the individual scans could be referenced to each other and combined into a single composite point cloud. Sparse returns were collected along the bottom of the manure pit because standing water has a tendency to scatter the light pulses from the sensor.

### *sUAS*

The properties of the sUAS flight at this location are presented in Table 3. A total of 37 images were taken at a resolution of 3.14 cm/pixel over an area of 2.33 hectares. The weather conditions during this flight were not ideal, with winds gusting as high as 9 m/s (20 mph). As a result, perpendicular flight lines, shown in Figure 9, were programmed to ensure sufficient imagery overlap. The variability seen in these flight lines is a direct result of the high winds. The level of imagery overlap obtained during this flight is displayed in Figure 10. High overlap is evident in the middle of the surveyed area, which corresponds to the location of the manure pit. No GCPs were used during this mission due to the lack of access to a GPS receiver.

*Table 3: Properties of Shelburne sUAS Flight*

<b>Image Count</b>	<b>Resolution (cm/pixel)</b>	<b>Surveyed Area (ha)</b>
37	3.14	2.33

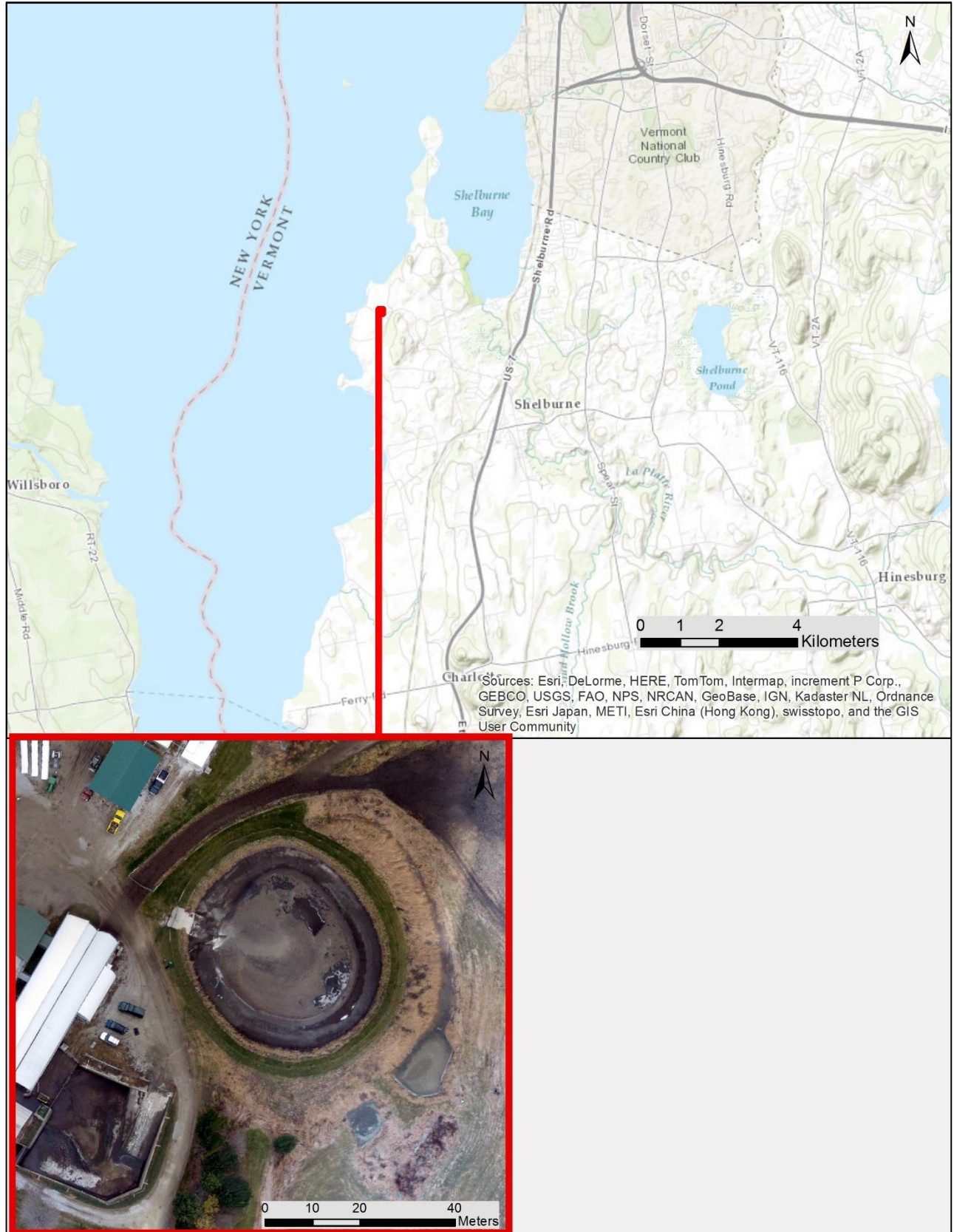
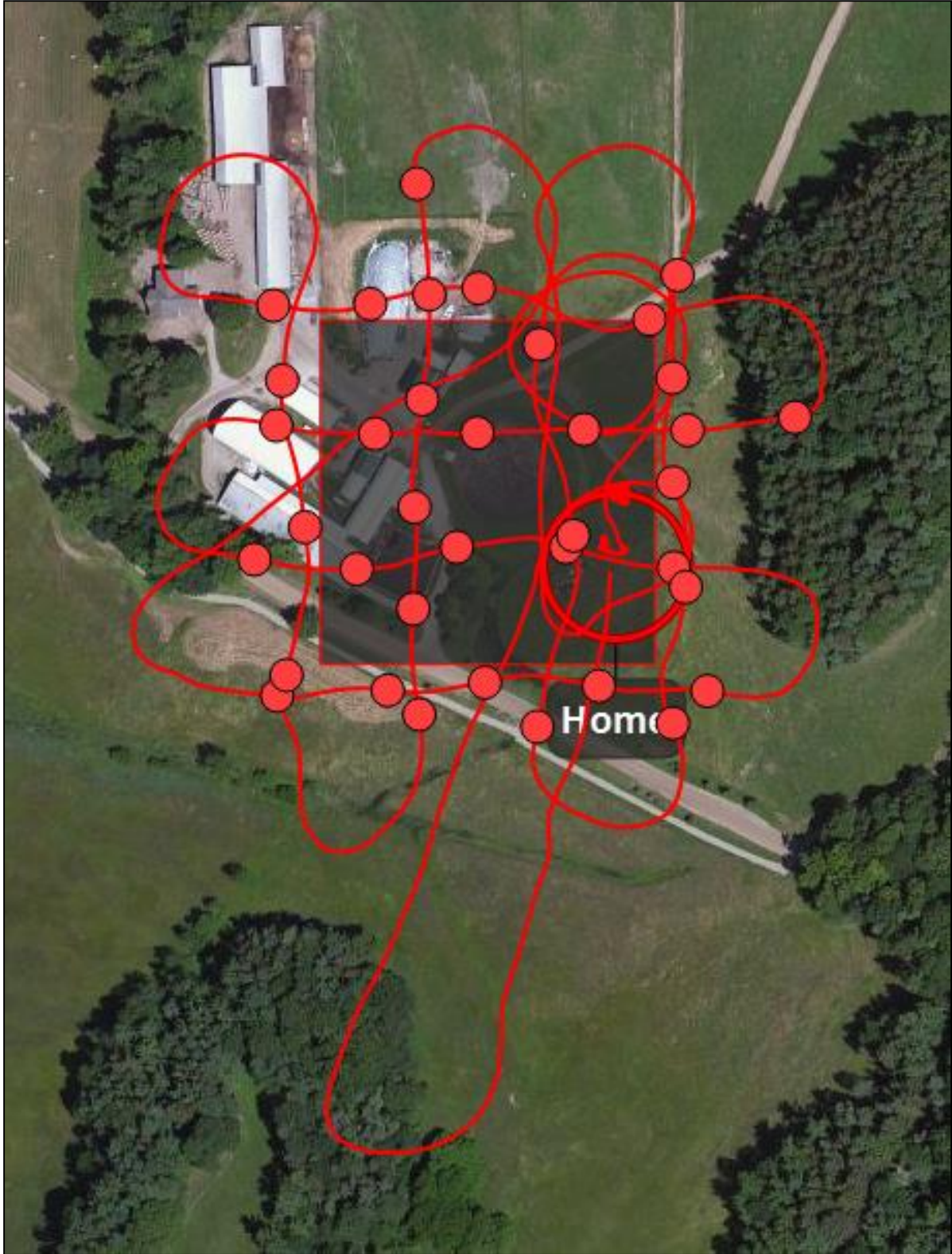
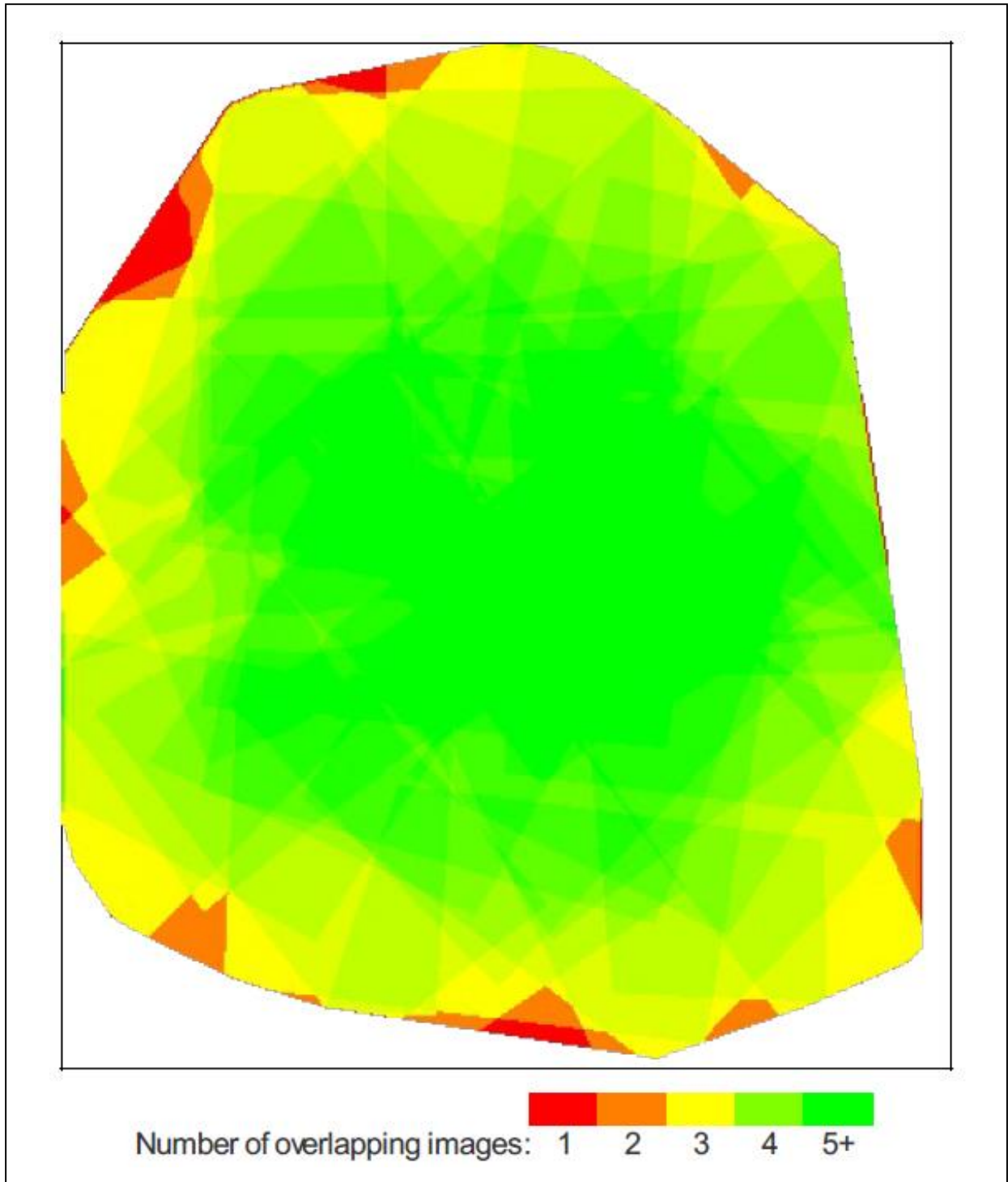


Figure 8: Location of manure pit in relation to Shelburne, VT



*Figure 9: sUAS flight lines for manure pit mission*



*Figure 10: Overlap of sUAS imagery for manure pit mission*

## Data Processing

### Terrestrial LiDAR

Composite point clouds of the collected terrestrial LiDAR data were created using the RIEGL RiSCAN PRO software package. For both surveyed features, the composite point cloud incorporated all of the returns of the scans undertaken at each site. The composite point clouds were exported to LAS files with metric coordinates in an arbitrary reference frame, as the export process resulted in the loss of coordinate system information. Due to this limitation, it was not possible to spatially overlay the sUAS and LiDAR data sets for direct comparison. These LAS files were imported into Quick Terrain Modeler (QTM) and cropped to the general location of each feature to reduce processing time. Extraneous returns above the stockpile and below the manure pit were filtered with clipping planes in QTM.

The cropped and clipped point clouds were exported to LAS files and individually re-imported into QTM as a QTT (gridded surface) to create an interpolated digital surface model. The characteristics of the point clouds and the import settings used to create each DSM are displayed in Table 4. The top and bottom images in Figure 11 respectively show the cropped point cloud and interpolated DSM of the stockpile. Note the absence of returns for the top of the stockpile in the point cloud and the resulting interpolated surface in the DSM. The composite manure pit point cloud and interpolated DSM are respectively displayed as the top and bottom image in Figure 12. Compare the sparse returns evident in the point cloud to the interpolated surfaces of the pit.

*Table 4: Interpolation settings for terrestrial LiDAR point clouds*

	<b>Morrisville Stockpile (Site 1)</b>	<b>Shelburne Manure Pit (Site 2)</b>
<b>Total points</b>	2,341,193	7,589,971
<b>Estimated ground sampling distance (m)</b>	0.036	0.018
<b>Grid sampling (m)</b>	0.036	0.018
<b>Fill method</b>	Adaptive triangulation	Adaptive triangulation
<b>Algorithm</b>	Mean Z	Mean Z
<b>Antialiasing</b>	Enabled	Enabled

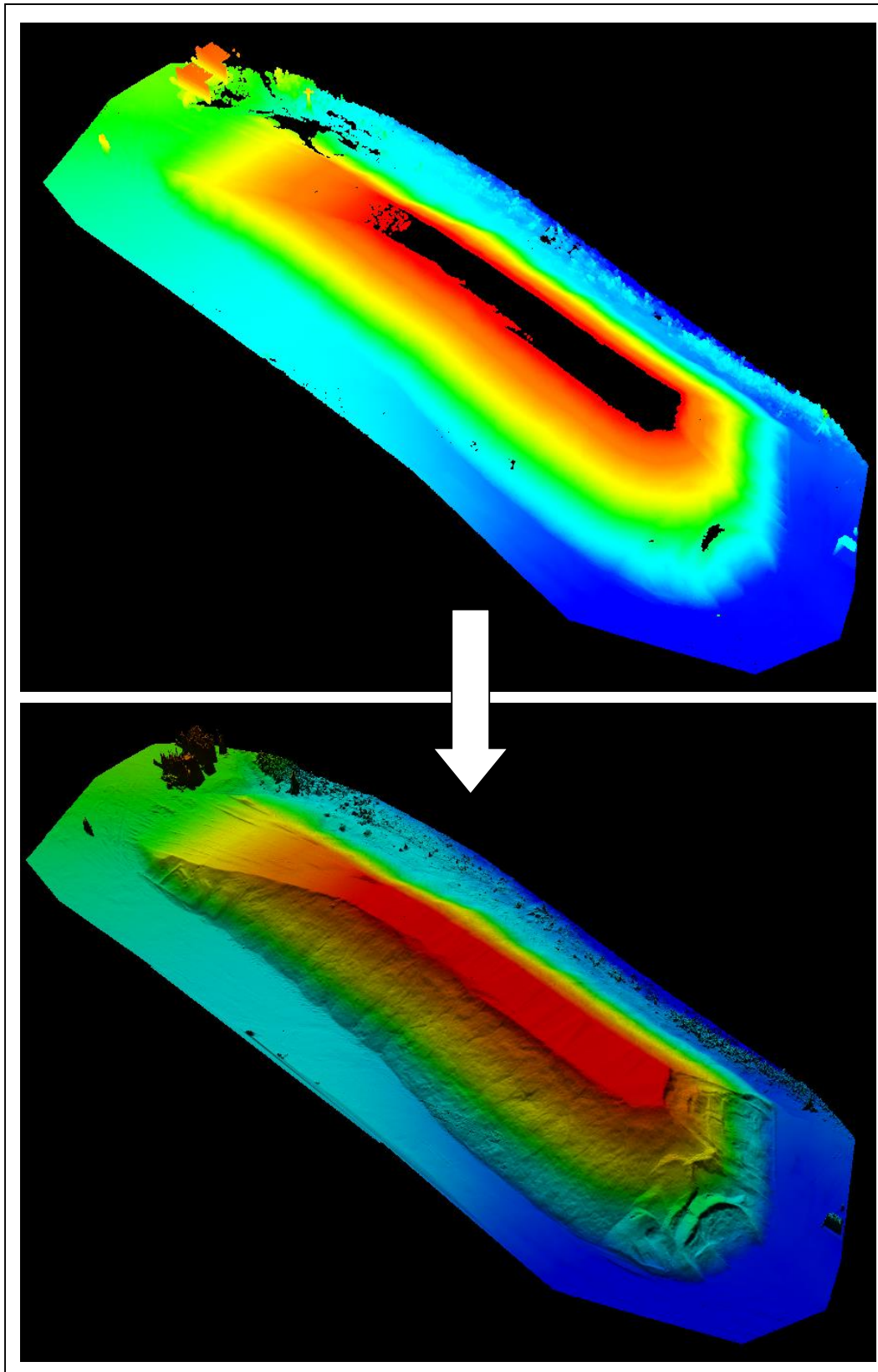


*Figure 11: Terrestrial LiDAR point cloud and interpolated DSM (stockpile)*

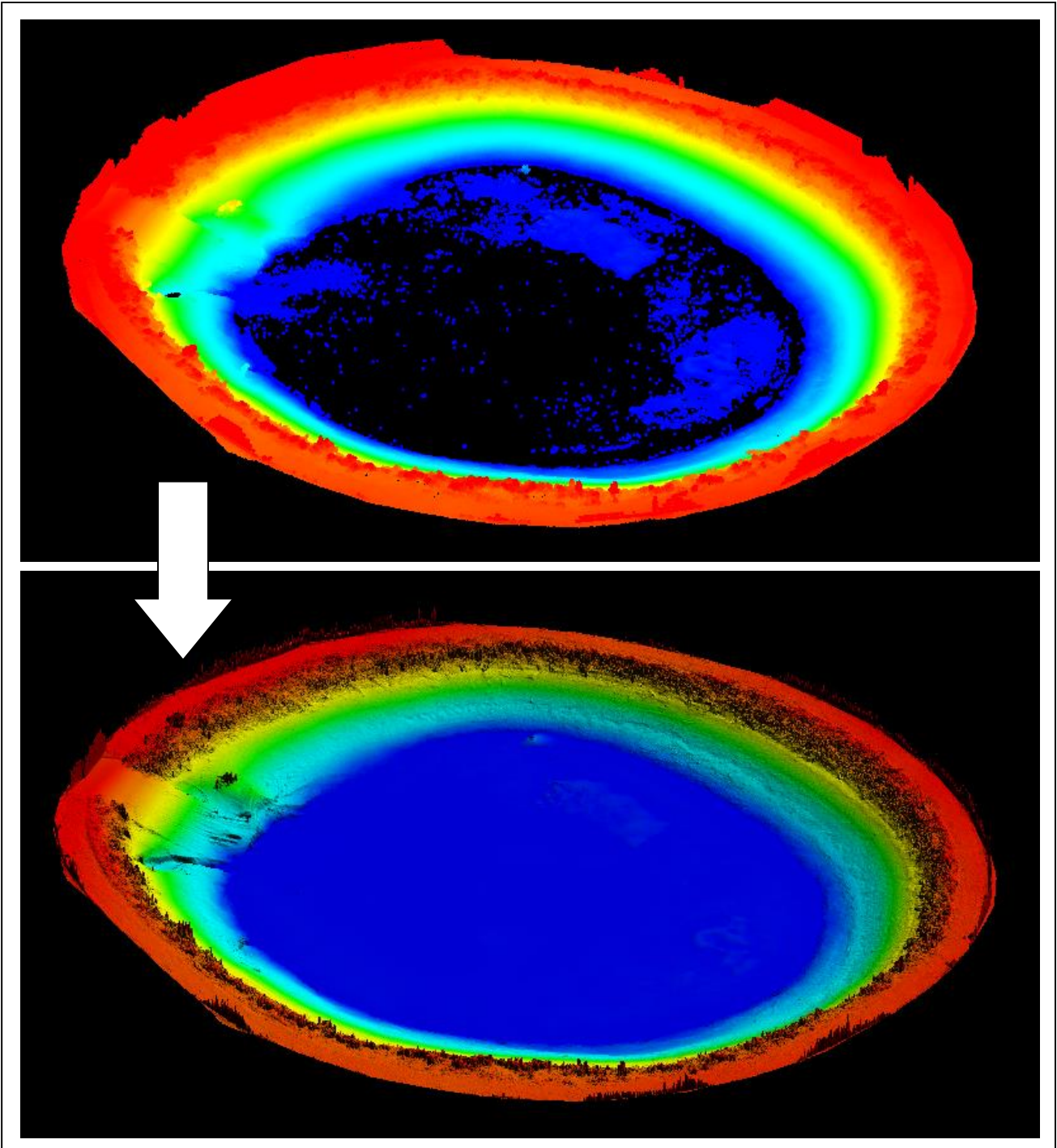


*Figure 12: Terrestrial LiDAR point cloud and interpolated DSM (manure pit)*

## sUAS

Project files for the two missions were created using eMotion2 and imported into SenseFly's PostFlight Terra 3D software, which was used to create a true-color orthomosaic, DSM, and colorized point cloud from the imagery and GPS data collected during each eBee mission. This software, included with the eBee, uses built-in algorithms to create a composite of the images captured during a flight and utilizes multi-view stereoscopic techniques to create and filter a point cloud. The points created in this process are assigned color values that correspond to the orthomosaic, resulting in the creation of a true-color 3D model. Local processing settings specified high tolerance algorithms to create the best possible resolution and 3D point density. These products are automatically exported to the same folder that the project file is stored. The orthomosaic and DSM are generated as rasters with a GeoTIFF file extension, while the point cloud is exported to a LAS file.

Prior to processing in PostFlight, GCP locations were integrated into the stockpile project data by entering their coordinates (refer to Table 1) and visually selecting their locations in all images in which they appeared. The PostFlight Terra GCP editor software interface used for this process is shown in Figure 13. The coordinates of the four GCPs used in the stockpile study site are tabulated in the upper portion of this image. The green number to the left of each GCP represents the number of images that capture this point. To the left is the list of all images taken during the mission. The preview pane in the bottom of the figure is used to digitize the location of a GCP within an image. Refer to the Standard Operating Guidelines attached as Appendix F for additional detail about GCP integration. This process was not carried out for the manure pit data because GCPs were not identified during the mission.



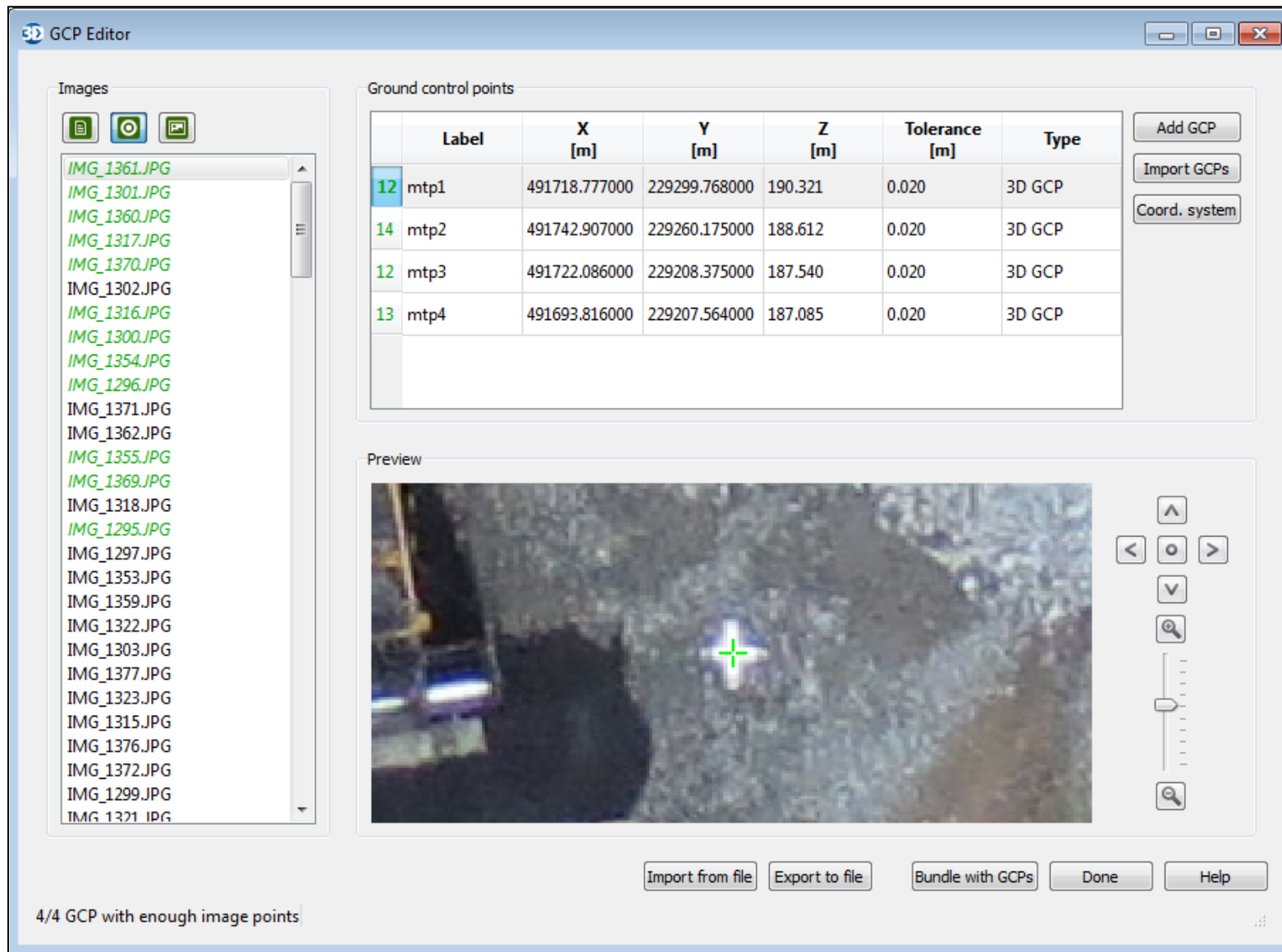
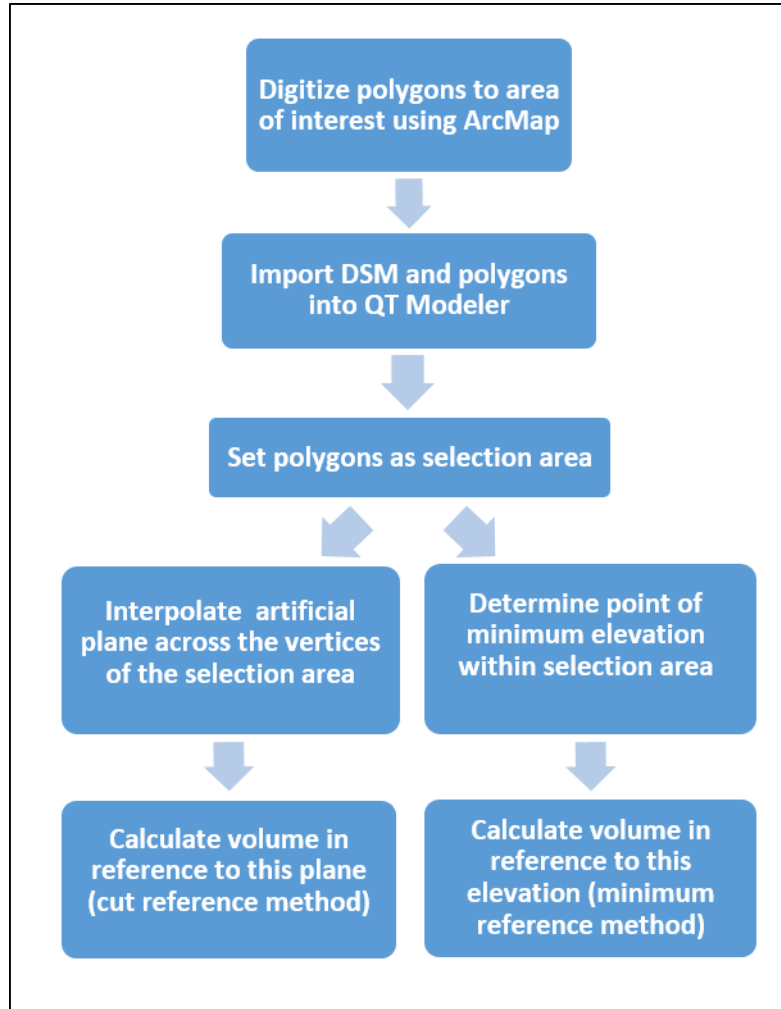


Figure 13: PostFlight Terra GCP Editor

## Volume Calculations

From the generated 3D surface models, two methods were utilized to calculate the volume of the stockpile and manure pit. For this assessment, the volume of the stockpile was defined as the volume of the feature above its apparent base and for the manure pit was defined as the volume of void space below the ring of vegetation. A process diagram for the volume calculations is presented in Figure 14.



*Figure 14: Volume calculation process diagram*

The minimum reference method, shown in Figure 15, was used to determine volume above a reference plane (i.e. datum) corresponding to the minimum elevation of the selection area. The 'Find lowest point in area' tool within the QT Modeler software package locates the minimum elevation

within a selected area. The ‘Volume Calculation’ functionality of QTM calculates the volume of the 3D model in relation to the horizontal reference plane.

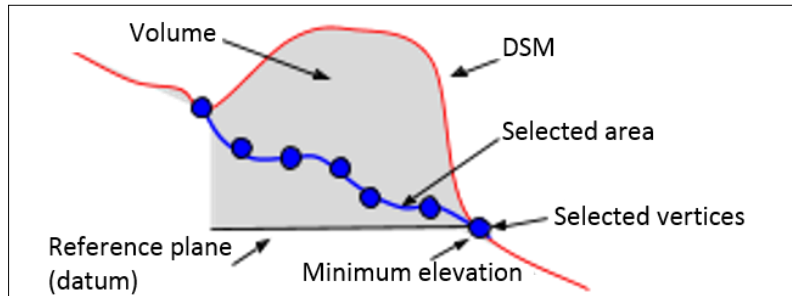


Figure 15: Cross section of minimum reference method<sup>1</sup>

Volume can also be determined using the cut reference method, in which an artificial surface is created by interpolating across all vertices of a selection area. A diagram of this method is presented in Figure 16. QT Modeler’s ‘Smooth Area’ tool was used to interpolate a plane across the extent of a vector polygon. The ‘Volume Calculation’ function in QTM calculates the volume of the 3D model relative to this interpolated reference plane.

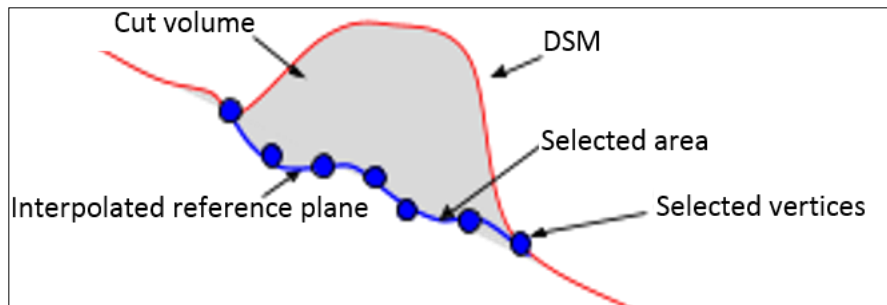


Figure 16: Cross section of cut reference method<sup>1</sup>

Typically, the cut reference method will yield estimates of volume that are less than those determined by the minimum reference method. Minimum reference may be applicable to scenarios in which a roadway has a known and constant elevation. This method also allows some flexibility because any arbitrary elevation can be specified to act as the reference plane. Cut reference would be more valid

<sup>1</sup> SenseFly: Measuring (<https://www.sensefly.com>)

for complex features, including sections of road with intermediate or steep grades, as well as stream and road banks.

## **sUAS**

Polygons representative of each feature were digitized in ArcMap using the orthomosaic images as a reference. These polygons were digitized to the perimeter of the stockpile and the perimeter of the manure pit below the ring of vegetation. Eight GIS technicians created 30 unique polygons for each feature to check for statistical validity. These polygons are overlaid on the stockpile orthomosaic in Figure 17 and on the manure pit orthomosaic in Figure 18. Note the variation between individual polygons for both locations.

The DSM and the digitized polygons were imported into QT Modeler. Minimum and cut reference volumes were calculated for the selection area defined by each individual polygon. The minimum reference elevation of the stockpile was defined as the lowest point within the polygon selection area. Due to the inverse geometry of the manure pit, the minimum reference elevation for this feature was defined as the highest point within the selection area. This allows for accurate calculation of the void volume.

To determine cut volume, QT Modeler's 'Smooth Area' tool was used to create an interpolated plane for the DSM across the extent of the defined selection area. This process is shown in Figure 19 for the stockpile and in Figure 20 for the manure pit. Note that the interpolated surfaces are not of constant elevation. The stockpile volume was calculated in QTM as the volume of the DSM above this interpolated plane. The volume of the manure pit was calculated as the volume of void below this plane.

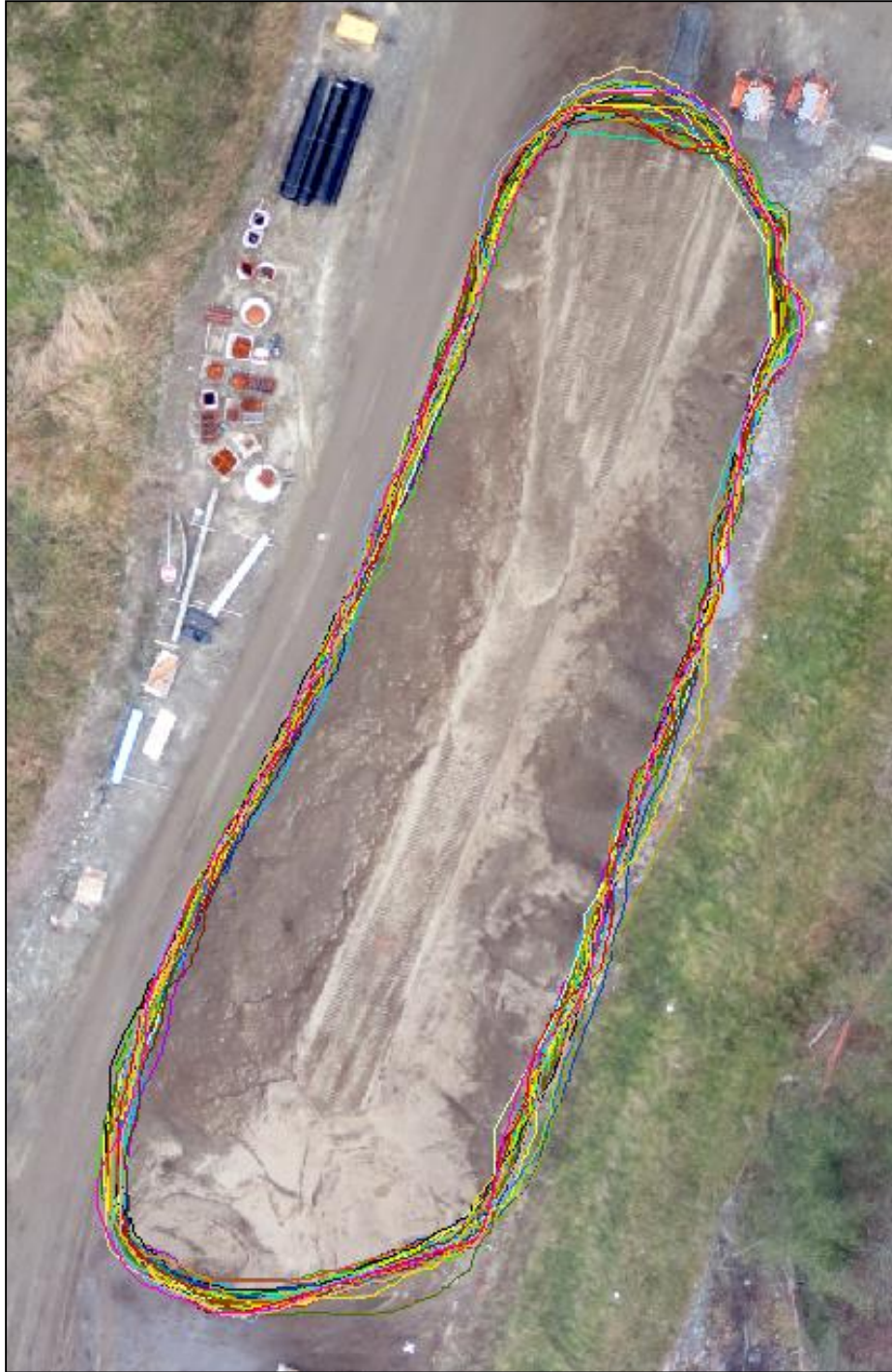


*Figure 17: Superposition of 30 unique stockpile base polygons (sUAS)*



*Figure 18: Superposition of 30 unique manure pit base polygons (sUAS)*

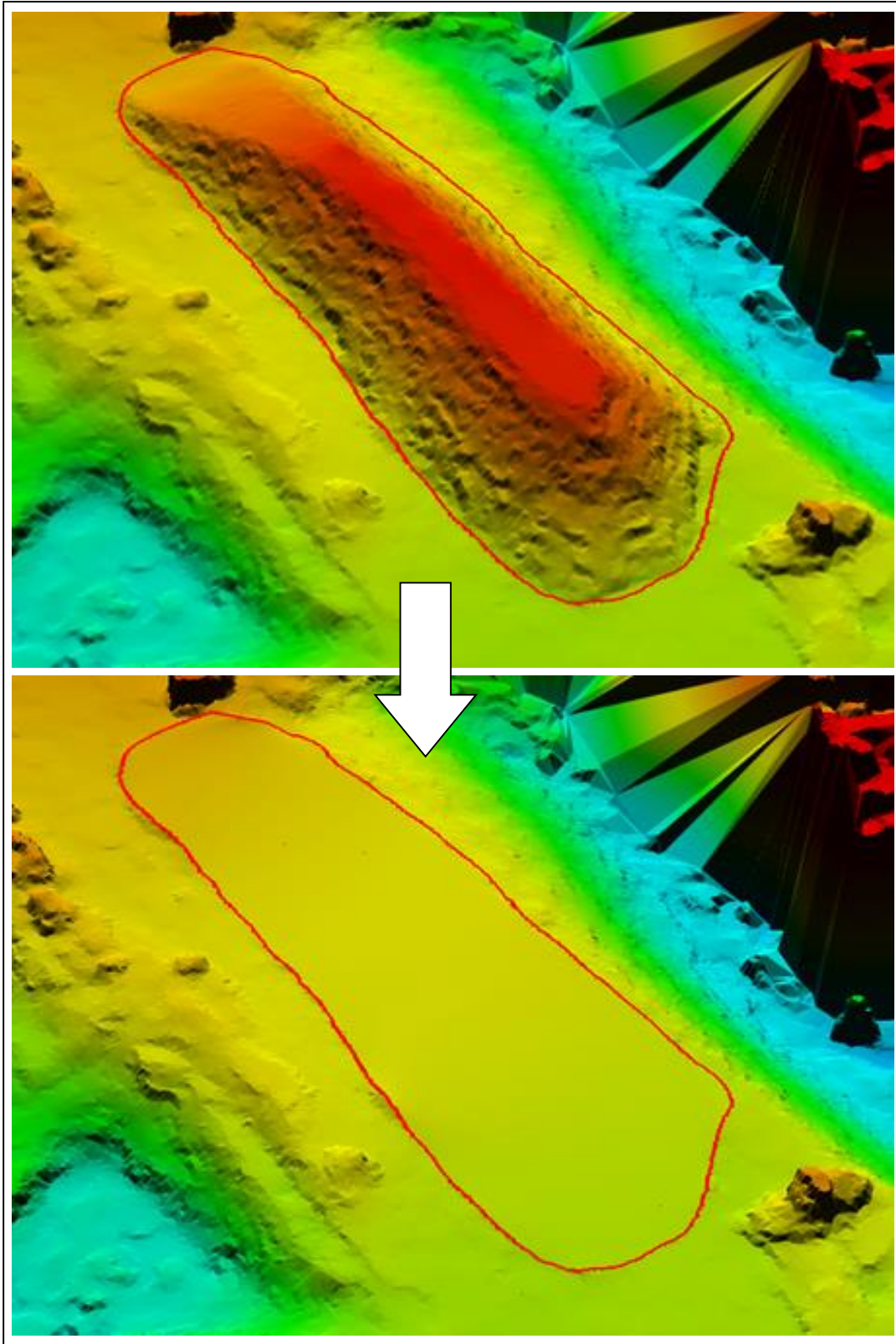


*Figure 19: Interpolation of stockpile cut reference plane (sUAS)*

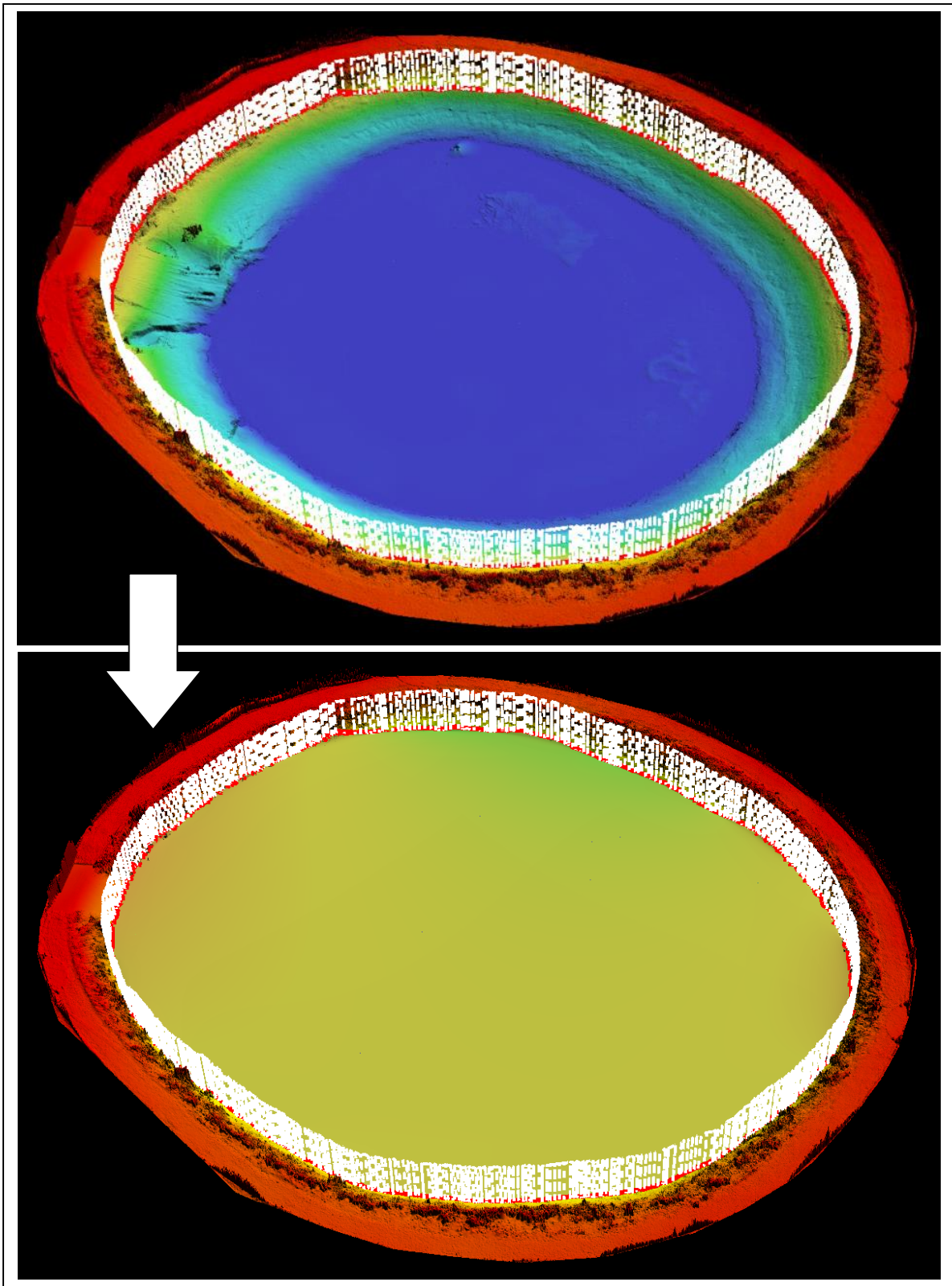


*Figure 20: Interpolation of manure pit cut reference plane (sUAS)*



### *Terrestrial LiDAR*

The DSM created from the LiDAR point cloud was imported as an ArcMap layer and manual digitization techniques were used to create 2D polygon shapefiles around the base of the stockpile and around the vegetation ring of the manure pit. Again, eight GIS technicians created a total of 30 unique polygons for each feature. These polygons are overlaid on the stockpile DSM in Figure 21 and the manure pit DSM in Figure 22. For both locations, the polygon vectors and the GeoTIFF DSM were imported into QTM and the extent of each vector layer was set as the selection area. Cut and minimum reference volumes for the LiDAR DSM were determined using the same workflow as the sUAS calculations. The cut reference interpolation process is shown in Figure 23 for the stockpile and Figure 24 for the manure pit.

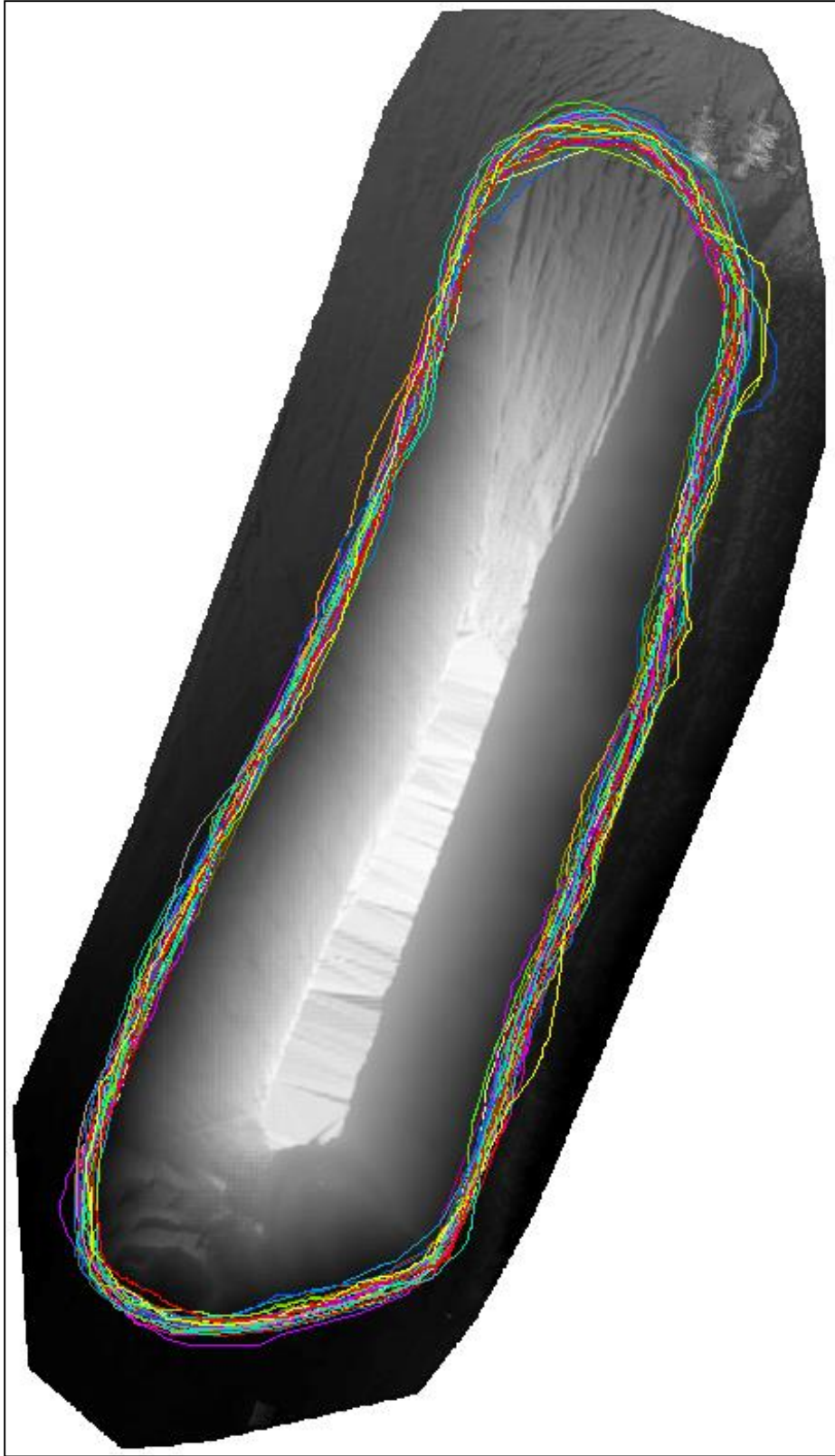


*Figure 21: Superposition of 30 unique stockpile base polygons (terrestrial LiDAR)*

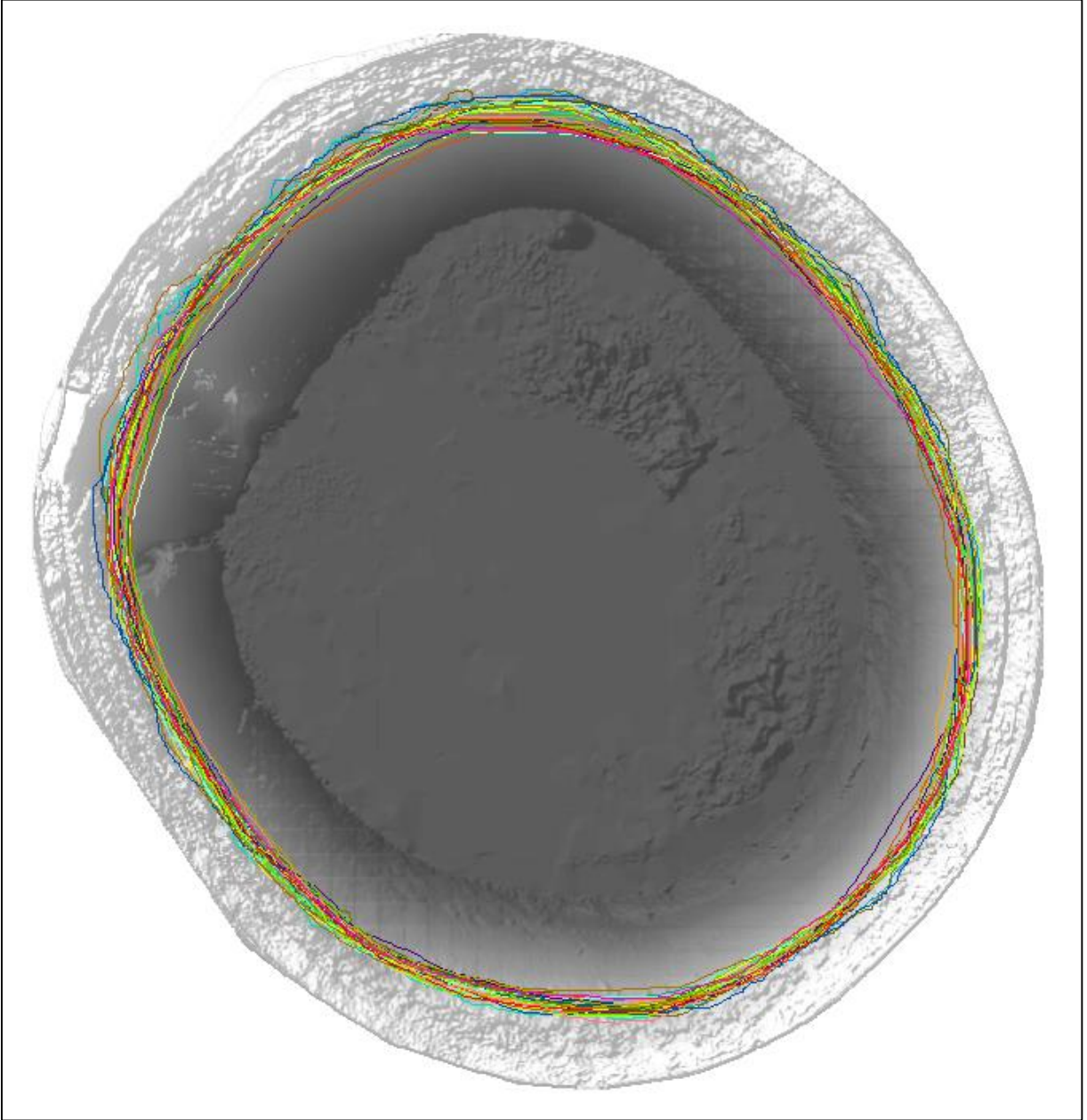


*Figure 22: Superposition of 30 unique manure pit base polygons (terrestrial LiDAR)*

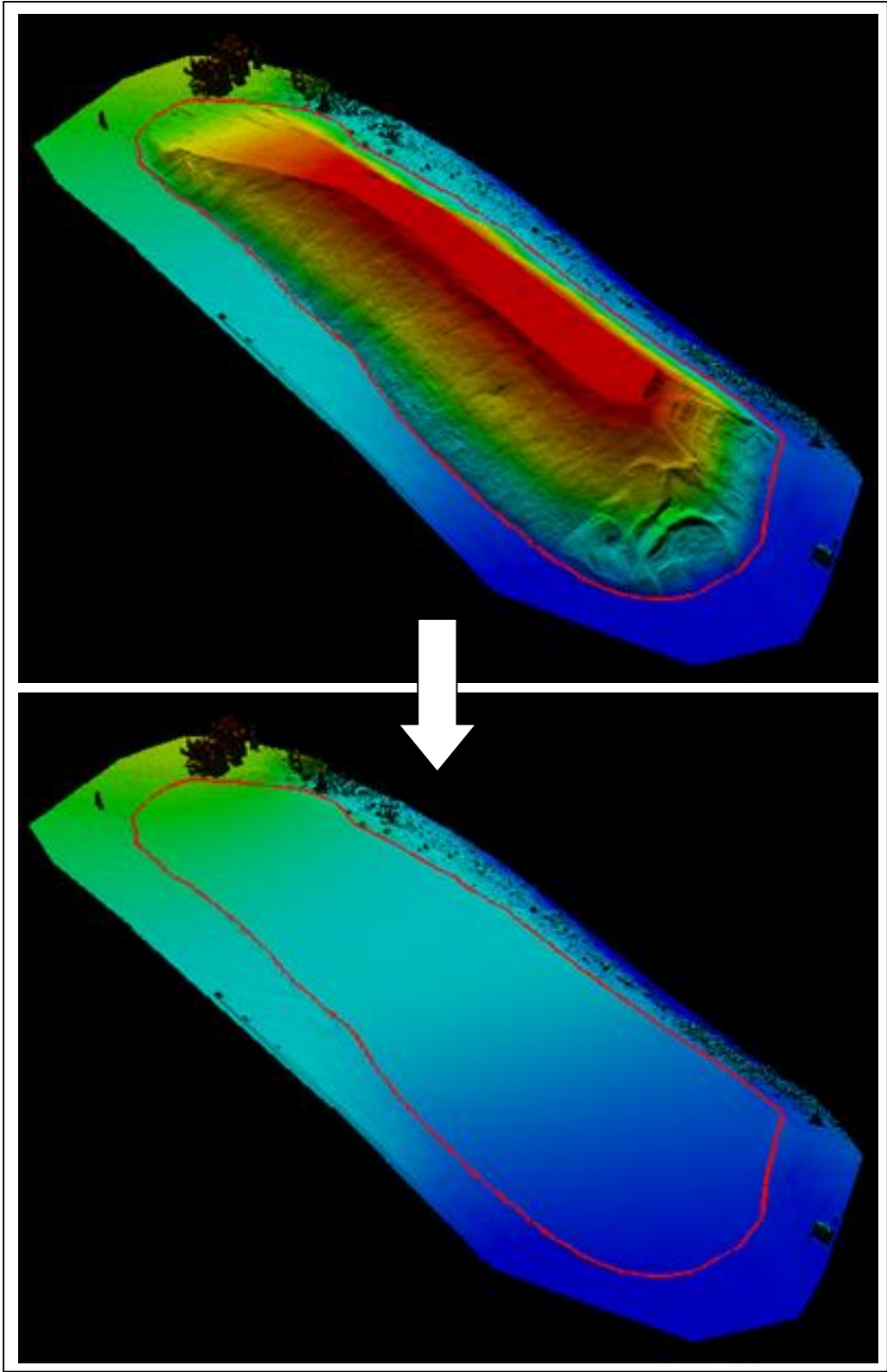


*Figure 23: Interpolation of stockpile cut reference plane (terrestrial LiDAR)*

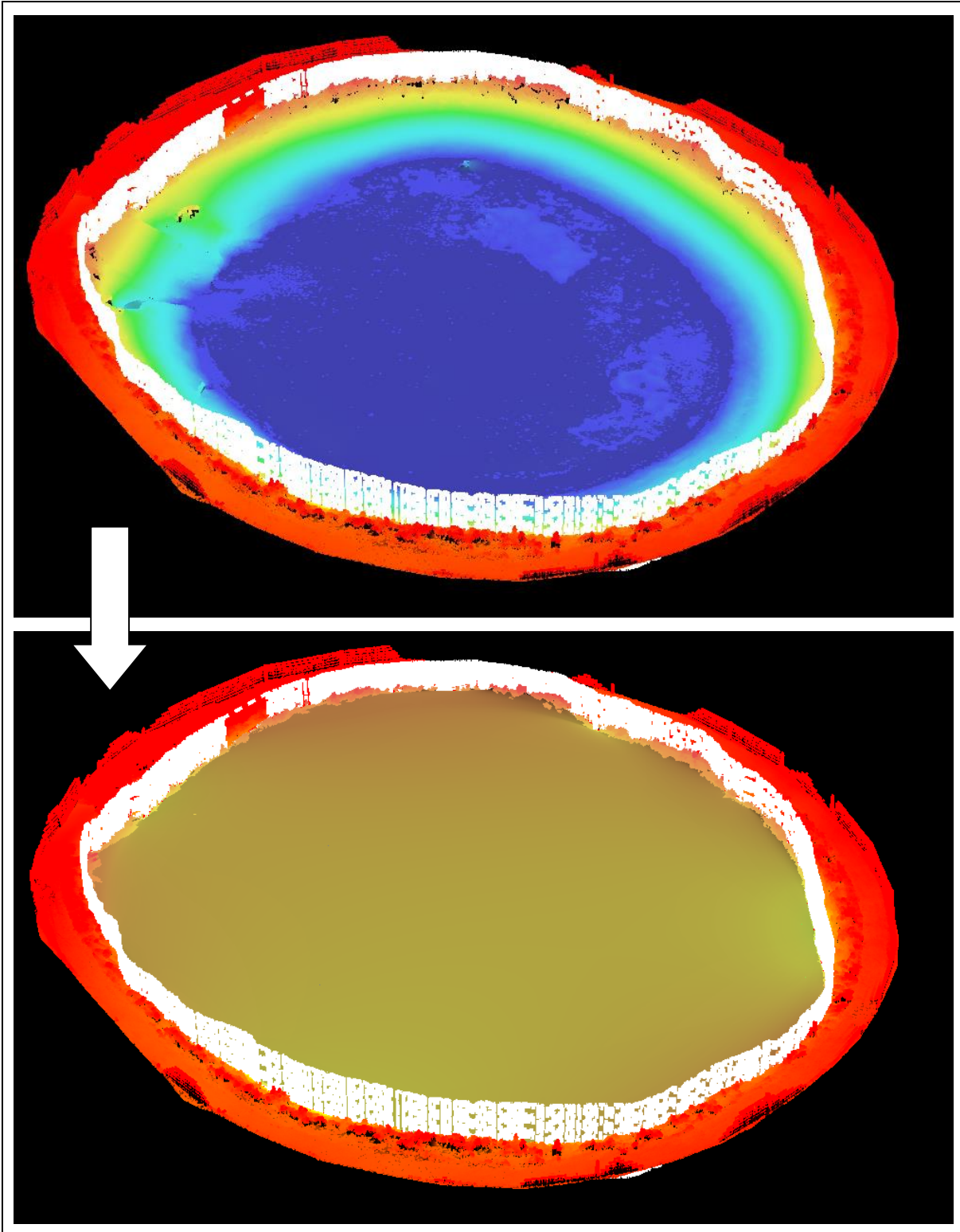


*Figure 24: Interpolation of manure pit cut reference plane (terrestrial LiDAR)*

## Results

The approximate data collection and post-processing times for the sUAS and terrestrial LiDAR platforms are displayed in Table 5. Data collection with the sUAS at both study sites was significantly faster in comparison to the terrestrial LiDAR sensor, although the creation of digital surface models from the sUAS data was a slower process. The times required to perform the actual volume calculations were not tabulated because they were the same for each platform. These results show that the sUAS offers substantial time savings for the end-to-end volume estimation process. In addition, the estimated training time for the terrestrial LiDAR sensor is one week, while a sUAS operator can be trained in just one to two days.

*Table 5: Time estimates for data collection and post-processing (hours)*

	<b>Morrisville Stockpile (Site 1)</b>		<b>Shelburne Manure Pit (Site 2)</b>	
	<i>sUAS</i>	<i>Terrestrial LiDAR</i>	<i>sUAS</i>	<i>Terrestrial LiDAR</i>
Data collection	0.75	4	0.5	3
Data processing	4	2	3	2
<b>Total time</b>	4.75	6	3.5	5

### Stockpile Volume

Summary statistics of the stockpile volumes are presented in Table 6. The complete results can be found in Appendix A. The mean volumes and standard deviations (STDEV) are tabulated in cubic meters and the relative standard deviation (RSD) is expressed as a percentage. “Relative difference” expresses the variation in mean volume between the sUAS and terrestrial LiDAR sensor. This difference is also presented as “Relative error” in percent.

For the minimum reference method, deviations in volume for both platforms are small, which suggests that the minimum elevation within the digitized polygons was consistent. The difference in calculated volume between the two platforms for this method is less than 22 m<sup>3</sup>, which is less than a one percent difference. This suggests high confidence in the accuracy of the sUAS.

Although the same selection area polygons were used for both the cut and minimum reference calculations, the relative standard deviations were larger when calculating cut reference volumes. This is

likely a result of the variations in the polygons as shown previously in Figure 17 and Figure 21. The difference in cut reference volume between the sUAS and LiDAR data is less than 100 m<sup>3</sup>, which corresponds to an error of 3.72%.

Table 6: Results of stockpile volume calculations

Platform	Minimum reference (m <sup>3</sup> )			Cut reference (m <sup>3</sup> )		
	Mean	STDEV	RSD	Mean	STDEV	RSD
Terrestrial LiDAR (n=30)	3761.33	64.33	1.71%	2595.09	90.7	3.49%
sUAS (n=30)	3782.64	69.03	1.82%	2691.65	56.4	2.10%
Relative difference	21.31			96.55		
Relative error	0.57%			3.72%		

## Manure Pit Volume

Summary statistics for the manure pit volumes are presented in Table 7. The complete results for the individual polygons can be found in Appendix B. The mean volumes are displayed as positive numbers for ease of interpretation but represent the void volume of this feature.

For the minimum reference method, the relative standard deviations from the mean volumes of both platforms are under 2%. This indicates that the maximum elevation of the DSM within each of the digitized polygons was consistent. The sUAS underestimated the volume of void space by nearly 600 m<sup>3</sup>, which corresponds to a relative error of nearly 16%.

The results of the cut reference calculations show that both platforms have moderate deviations from their mean volumes. The relative standard deviation for the LiDAR sensor is nearly 8%. It is likely that this is a result of variations in the digitized polygons because the ring of vegetation around the manure pit was difficult to identify in the DSM used as a digitizing reference. Compared to the LiDAR sensor, the sUAS underestimated the void volume by 24 m<sup>3</sup>. This corresponds to an absolute relative error of 1.15%.

Table 7: Results of manure pit volume calculations

Platform	Minimum reference (m <sup>3</sup> )			Cut reference (m <sup>3</sup> )		
	Mean	STDEV	RSD	Mean	STDEV	RSD
<i>Terrestrial LiDAR</i> (n=30)	3638.95	416.24	1.71%	2081.63	159.36	7.66%
<i>sUAS</i> (n=30)	3068.54	281.36	1.82%	2057.63	93.10	4.52%
<i>Relative difference</i>	-570.41			-24.00		
<i>Relative error</i>	-15.68%			-1.15%		

As expected, the volumes calculated using the minimum reference method were greater than the volumes determined with the cut reference method. For both the stockpile and the manure pit, this difference was on the order of 1000 m<sup>3</sup>, which indicates that the base of the pile was not at a constant elevation. The cut reference volumes may be considered the more accurate estimation for this scenario. However, the appropriate method of volume calculation relies heavily on the topology of the surveyed area and the goals for volumetric estimation. In the case of a damaged roadway, the best approach for determining fill volumes may be to calculate the void area below the known constant elevation of the road surface.

## Conclusions

The results of this thesis research demonstrate that a lightweight commercial sUAS has the potential to provide estimates of volume with enough accuracy for disaster response and recovery. The 3D surface models generated from aerial images captured by the SenseFly eBee are comparable to data collected by a RIEGL VZ1000 Terrestrial Laser Scanner. Volume estimations by sUAS using the cut reference method are within 4% of the values calculated with LiDAR data for two types of features. Clearly, this system is able to provide estimates of volume with more accuracy than “back of the envelope calculations” by a field engineer. In addition, the lightweight sUAS platform allows for on-site data collection to be carried out in a fraction of the time of a LiDAR scan or traditional survey. Cost reduction and ease of use are added benefits of sUAS systems, as the SenseFly eBee sUAS used in this research is approximately a tenth of the price of the RIEGL VZ1000 Terrestrial Laser Scanner and does not require the same level of technical skill to collect and process data. The ability to remotely survey an



area from a secure nearby location is also an advantage over more traditional techniques that require a crew on the ground. Applied to a post-disaster scenario, this inherent capability of UAS could reduce potential safety risks and hazards for members of the agency involved in the response. In conjunction with the ability of these systems for rapid and repeated deployment in the immediate aftermath of a disaster event, sUAS can allow disaster response to be carried out in a more immediate timeframe with increased precision and reduced cost.

## Acknowledgements

I would like to thank the USDOT and Mr. Caesar Singh for providing funding for this research, as well as Dr. Jeff Frolik and Hanna Anderson for their help in acquiring LiDAR data. Also, a big thank you to my faculty advisors for all their guidance and the staff of the SAL and TRC for allowing me this incredible research opportunity.

## Literature Review

Adams, S.; Friedland, C. (2011). A Survey of Unmanned Aerial Vehicle (UAV) Usage for Imagery Collection in Disaster Research and Management. *Ninth International Workshop on Remote Sensing for Disaster Response*.

Federal Aviation Administration (FAA) (2013). *Unmanned Aircraft Systems (UAS)*.  
<[http://www.faa.gov/news/fact\\_sheets/news\\_story.cfm?newsId=14153](http://www.faa.gov/news/fact_sheets/news_story.cfm?newsId=14153)>

Harwin, S.; Lucieer, A. (2012). Assessing the Accuracy of Georeferenced Point Clouds Produced via Multi-View Steopsis from Unmanned Aerial Vehicle (UAV) Imagery. *Remote Sensing*, 4, 1573-1599.

Heuchel, T. A. Kosteli, C. LeMaire, and D. Wild. (2011). *Towards a Next Level of Quality DSM/DTM Extraction with MATCH-T*. <<http://www.ifp.uni-stuttgart.de/publications/phowo11/200Heuchel.pdf>>

Hodgson, A.; et al. (2010). Using Unmanned Aerial Vehicles for Surveys of Marine Mammals in Australia: Test of Concept. *Australian Marine Mammal Centre*.

Laliberte, A.; Herrick, J.; Winters, C. (2010). Acquisition, Orthorectification, and Object-based Classification of Unmanned Aerial Vehicle (UAV) Imagery for Rangeland Monitoring. *Photogrammetric Engineering & Remote Sensing*, 76, 661-672.

Madrigal, A. (2011). Inside the Drone Missions to Fukushima. *The Atlantic*.  
<<http://www.theatlantic.com/technology/archive/2011/04/inside-the-drone-missions-to-fukushima/237981>>

Mander, D. (2012). Unmanned Drones in Conservation. *International Anti-Poaching Foundation* (2012).

Murphy, R. (2011). Have Robots Been Used in Previous Earthquakes? *Center for Robot-Assisted Search and Rescue, Texas Agricultural and Mechanical University*.

Neitzel, F.; Klonowski, J. (2011). Mobile 3D Mapping With a Low-Cost UAV System. *International Archives of the Photogrammetry, Remote Sensing, and Spatial Information Sciences*, 38, 1-6.

Petcoff, R. (2010). Global Hawk Collects Reconnaissance Data During Haiti Relief Efforts. *United States Air Force Departmental Publishing Office*.

Snitch, T. (2013). Entrepreneurial Approaches to Protecting Highly Endangered Wildlife: Saving Rhinos with Math, Drones and Satellites. *University of Maryland*.

Troy, A. and O'Neil-Dunne, J. (2013). *Rapid Exploitation of Commercial Remotely Sensed Imagery for Disaster Response & Recovery*. University of Vermont Transportation Research Center (TRC) and Spatial Analysis Lab (SAL).

## Appendix A: Stockpile Volume Data

*Table 8: sUAS stockpile volumes*

Polygon ID	Min Z (m)	Volume (m <sup>3</sup> )	
		Min Reference	Cut Reference
UAS01	187.26	3889.62	2670.03
UAS02	187.38	3774.83	2740.91
UAS03	187.39	3735.75	2677.84
UAS04	187.32	3852.92	2738.38
UAS05	187.32	3779.57	2666.17
UAS06	187.38	3711.83	2626.51
UAS07	187.32	3826.32	2730.82
UAS08	187.33	3818.44	2726.74
UAS09	187.39	3772.91	2772.74
UAS10	187.38	3766.27	2714.71
UAS11	187.33	3817.62	2736.77
UAS12	187.37	3780.55	2740.56
UAS13	187.29	3849.66	2724.78
UAS14	187.37	3747.22	2693.59
UAS15	187.27	3835.43	2694.86
UAS16	187.41	3677.13	2692.58
UAS17	187.39	3702.11	2601.77
UAS18	187.37	3741.46	2687.03
UAS19	187.36	3760.22	2687.93
UAS20	187.33	3746.79	2618.60
UAS21	187.39	3728.52	2651.96
UAS22	187.32	3771.34	2626.25
UAS23	187.41	3668.34	2551.94
UAS24	187.33	3766.20	2674.87
UAS25	187.47	3624.81	2579.74
UAS26	187.31	3860.31	2727.22
UAS27	187.30	3851.89	2724.83
UAS28	187.32	3828.63	2760.38
UAS29	187.26	3899.59	2748.09
UAS30	187.27	3893.06	2760.79
<b>Mean</b>	<b>187.34</b>	<b>3782.64</b>	<b>2691.65</b>
<b>stdev</b>	0.05	69.03	56.40
<b>RSD</b>	0.03%	1.82%	2.10%

Table 9: Terrestrial LiDAR stockpile volumes

Polygon ID	Min Z (m)	Volume (m <sup>3</sup> )	
		Min Reference	Cut Reference
LIDAR01	165.293	3591.80	2643.43
LIDAR02	165.173	3791.10	2681.31
LIDAR03	165.142	3759.05	2602.92
LIDAR04	165.116	3798.87	2652.58
LIDAR05	165.103	3852.24	2728.84
LIDAR06	165.181	3709.74	2539.34
LIDAR07	165.125	3846.15	2725.15
LIDAR08	165.183	3762.73	2582.72
LIDAR09	165.104	3775.00	2571.41
LIDAR10	165.12	3788.19	2618.52
LIDAR11	165.127	3809.52	2725.90
LIDAR12	165.203	3672.28	2566.15
LIDAR13	165.198	3714.46	2540.48
LIDAR14	165.18	3701.79	2598.03
LIDAR15	165.125	3755.25	2615.28
LIDAR16	165.101	3778.11	2469.60
LIDAR17	165.12	3775.53	2590.56
LIDAR18	165.128	3741.69	2429.93
LIDAR19	165.128	3764.35	2561.95
LIDAR20	165.169	3707.12	2461.39
LIDAR21	165.198	3669.96	2467.52
LIDAR22	165.139	3728.01	2491.25
LIDAR23	165.199	3660.45	2486.18
LIDAR24	165.12	3784.12	2584.43
LIDAR25	165.097	3805.79	2492.34
LIDAR26	165.173	3743.25	2650.10
LIDAR27	165.119	3816.32	2604.67
LIDAR28	165.125	3809.30	2707.53
LIDAR29	165.083	3889.26	2742.33
LIDAR30	165.102	3838.52	2720.92
<b>Mean</b>	<b>165.146</b>	<b>3761.33</b>	<b>2595.09</b>
<b>stdev</b>	0.045	64.33	90.70
<b>RSD</b>	0.03%	1.71%	3.49%

## Appendix B: Manure Pit Volume Data

*Table 10: sUAS manure pit volumes*

Polygon ID	Max Z (m)	Volume (m <sup>3</sup> )	
		Min Reference	Cut Reference
UAS01	48.54	3445.08	2167.08
UAS02	48.57	3,478.33	2,139.08
UAS03	48.22	3002.66	1961.84
UAS04	47.96	2658.26	1958.13
UAS05	48.57	3503.93	2299.25
UAS06	48.57	3496.19	2283.82
UAS07	48.57	3490.97	2175.13
UAS08	48.57	3481.06	2110.58
UAS09	48.03	2757.64	2093.89
UAS10	48.41	3255.28	2089.83
UAS11	48.08	2821.47	2072.30
UAS12	48.15	2914.58	2078.94
UAS13	48.18	2933.80	1947.23
UAS14	48.20	2971.81	2041.80
UAS15	48.03	2757.11	2050.74
UAS16	48.50	3352.85	2048.42
UAS17	48.35	3175.60	2106.23
UAS18	48.19	2953.44	1947.69
UAS19	48.15	2912.25	2052.90
UAS20	47.96	2658.27	2000.12
UAS21	48.33	3145.88	2014.68
UAS22	48.02	2741.62	1987.24
UAS23	48.19	2956.40	1925.96
UAS24	48.46	3314.43	1964.87
UAS25	48.28	3074.93	1945.16
UAS26	48.31	3133.37	1993.80
UAS27	48.02	2751.61	2054.48
UAS28	48.01	2733.57	2059.77
UAS29	48.40	3248.96	2035.48
UAS30	48.16	2934.74	2122.39
<b>Mean</b>	<b>48.26</b>	<b>3068.54</b>	<b>2057.63</b>
<b>stdev</b>	0.21	281.36	93.10
<b>RSD</b>	0.43%	9.17%	4.52%

Table 11: Terrestrial LiDAR manure pit volumes

Polygon ID	Max Z (m)	Volume (m <sup>3</sup> )	
		Min Reference	Cut Reference
LIDAR01	9.263	4059.33	2226.99
LIDAR02	8.59	3108.14	2026.36
LIDAR03	8.829	3405.64	1867.48
LIDAR04	8.703	3239.70	1886.50
LIDAR05	8.694	3273.34	2198.05
LIDAR06	8.906	3573.98	2271.99
LIDAR07	9.374	4210.74	2186.02
LIDAR08	8.325	2750.65	1932.04
LIDAR09	8.749	3300.76	1860.36
LIDAR10	9.001	3702.97	2241.17
LIDAR11	9.226	4012.70	2270.57
LIDAR12	9.269	4060.43	2229.05
LIDAR13	9.269	4091.85	2291.05
LIDAR14	8.41	2858.93	1869.71
LIDAR15	9.056	3758.71	2153.36
LIDAR16	8.694	3275.43	2166.09
LIDAR17	9.024	3726.44	2105.05
LIDAR18	9.269	4042.49	2087.58
LIDAR19	9.269	4055.48	2175.60
LIDAR20	9.269	4073.40	2290.04
LIDAR21	9.135	3859.10	2048.46
LIDAR22	9.269	4058.71	2188.06
LIDAR23	8.828	3413.17	1912.83
LIDAR24	9.024	3737.09	2137.88
LIDAR25	9.187	3966.35	2124.36
LIDAR26	9.135	3895.36	2192.75
LIDAR27	8.51	2972.40	1729.11
LIDAR28	8.743	3300.92	1906.82
LIDAR29	8.829	3420.88	1984.12
LIDAR30	9.263	3963.46	1889.40
<b>Mean</b>	<b>8.970</b>	<b>3638.95</b>	<b>2081.63</b>
<b>stdev</b>	0.295	416.24	159.36
<b>RSD</b>	3.29%	11.44%	7.66%

# Appendix D: Morrisville sUAS Flight Quality Report

## Quality Report



See *Quality Report Help* for detailed explanations. Generated with version 3.0.3

### Summary

Project:	21nov2013_morrisville30cm_crop
Processed:	2014-Feb-01 18:02:15
Camera name:	CanonIXUS127HS_4.3_4608x3456
Average Ground Sampling Distance (GSD):	3.25 cm
Area covered:	0.0381 km <sup>2</sup> / 3.8143 ha / 0.0147 sq. mi.
Image coordinate system:	WGS84
Ground Control Point (GCP) coordinate system:	NAD83 / Vermont
Output coordinate system:	NAD83 / Vermont
Processing type:	full (scale 1) aerial
Time for Initial Processing (without report):	27m:32s

### Quality Check

Images:	median of 33238 keypoints per image	✓
Dataset:	166 out of 166 images calibrated (100%), all images enabled	✓
Camera optimization quality:	0.45% relative difference between initial and final focal length	✓
Matching quality:	median of 6493 matches per calibrated image	✓
Georeferencing:	4 GCPs, 0.013 m	✓

### Preview

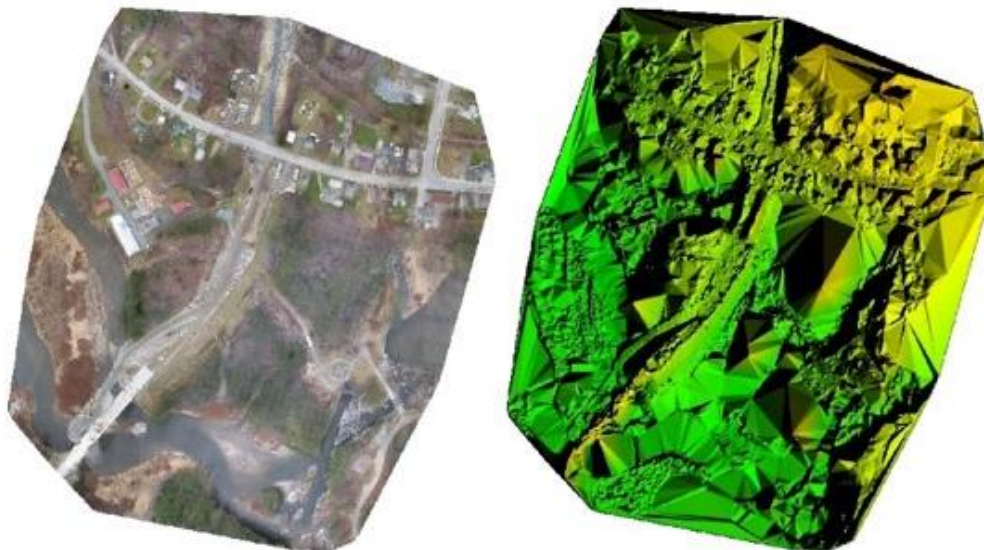


Figure 1: Ortho mosaic and the corresponding sparse digital surface model (DSM) before densification.

## Calibration details

Number of calibrated images:	166 out of 166
Number of geotagged images:	166 out of 166

### Geotag position

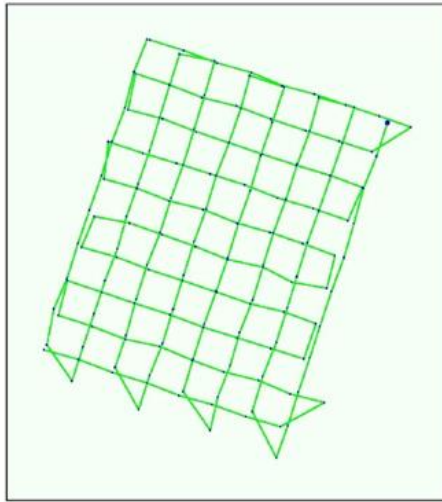


Figure 2: Top view of the geotags. The green line follows the geotags of the images in time starting from the large blue dot.

### Optimized camera position

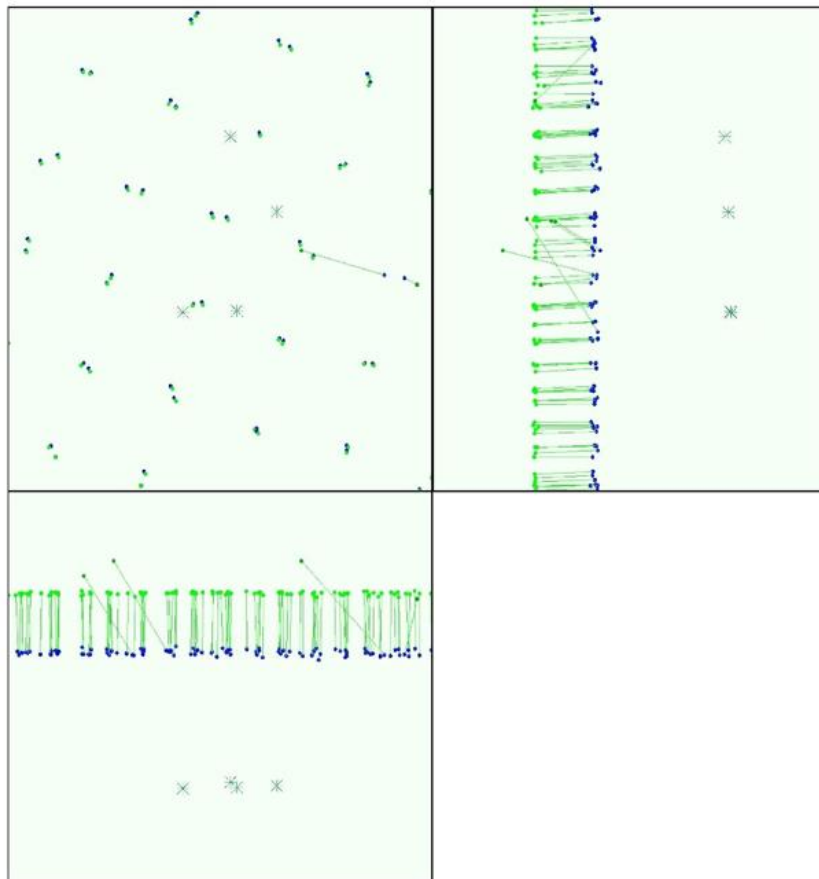


Figure 3: Offset between image geotags (blue dots) and optimized positions (green dots) as well as the offset between the GCPs positions (blue crosses) and their optimized positions (green crosses) in the top-view (XY plane), front-view (XZ plane) and side-view (YZ plane).



## Overlap

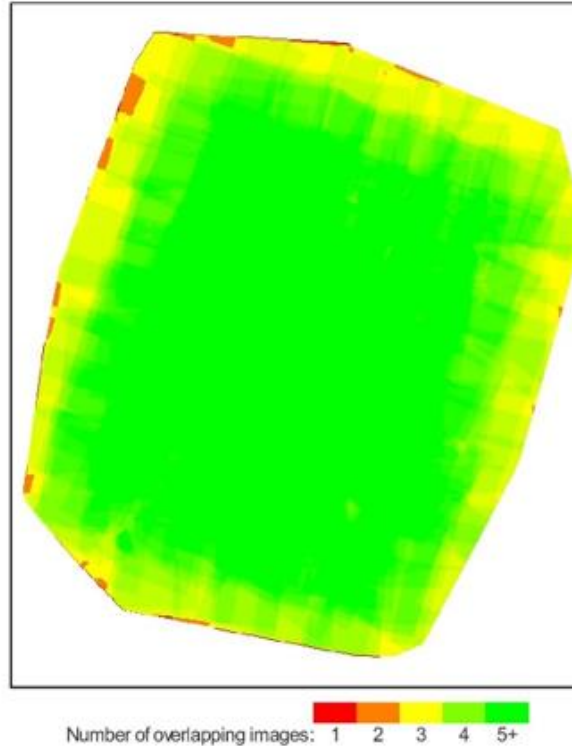


Figure 4: Overlapping score computed for each pixel of the orthomosaic. Red indicates areas where the overlap between the images is too low and could lead to poor results. For good quality results, the overlap should be over 5 images (green) for every pixel of the mosaic.

## Bundle Block Adjustment details

number total keypoint observations (automatic tie points) for bundle block adjustment	1082814
number total 3D points for bundle block adjustment	427759
mean reprojection error	0.191299 [pixels]

Internal Camera Parameters ⓘ CanonIXUS127HS\_4.3\_4608x3456. Sensor dimensions: 6.17 [mm] x 4.63 [mm]

EXIF ID: CanonIXUS127HS\_4.3\_4608x3456

	Focal length	Principal point x	Principal point y	R1	R2	R3	T1	T2
initial values	3270.925 [pix] 4.380 [mm]	2304.000 [pix] 3.085 [mm]	1728.000 [pix] 2.314 [mm]	-0.049	0.059	-0.036	0.000	-0.003
optimized values	3285.956 [pix] 4.400 [mm]	2372.392 [pix] 3.177 [mm]	1855.333 [pix] 2.484 [mm]	-0.040	0.033	-0.012	0.008	0.005

## 2D Keypoints Table

	Number of 2D keypoints per image	Number of matched 2D keypoints per image
Median	33238	6493
Mn	19303	189
Max	58081	11955
Mean	34244	6523

### 3D points from 2D keypoints matches

	Number of 3D points observed
In 2 images	334767
In 3 images	45458
In 4 images	18366
In 5 images	9732
In 6 images	6135
In 7 images	4159
In 8 images	3037
In 9 images	2071
In 10 images	1440
In 11 images	1030
In 12 images	726
In 13 images	456
In 14 images	237
In 15 images	101
In 16 images	28
In 17 images	15
In 18 images	1

### 2D Keypoints Graph

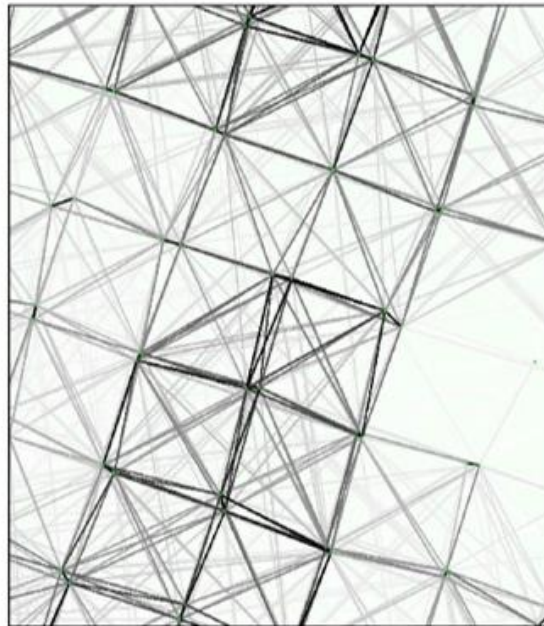


Figure 5: Top view of the geotags with a link between matching images. The darkness of the links indicates the number of matched 2D keypoints between the images. Bright links indicate low confidence and would require more overlap between the images or better quality images.

### Most visible 2D keypoints



Figure 6: Cropped area of 1 3D points arising from 18 2D keypoints. Each cropped area should represent the same 3D object.

## Geo-location and Ground Control Points

GCP name	tolerance [m]	error X [m]	error Y [m]	error Z [m]	projection error [pixel]	verified/ measured
3D GCP: mtp1	0.020	-0.002	-0.005	0.045	0.125	12 / 12
3D GCP: mtp2	0.020	-0.003	-0.003	-0.014	0.164	14 / 14
3D GCP: mtp3	0.020	0.004	-0.013	-0.038	0.271	12 / 12
3D GCP: mtp4	0.020	0.008	-0.013	0.008	0.236	13 / 13
Mean		0.001615	-0.008294	0.000356		
Sigma		0.004527	0.004420	0.030717		

Localisation accuracy of the individual GCP, their mean error distance and the mean errors in the three coordinate directions. The last column counts the number of images where the GCP has been measured (clicked on the images) and on how many of them have been automatically verified. 0 out of 0 GCPs have been labeled as inaccurate (see Figure below).

### Geotag variance

Geotag localisation variance	sigma m
Longitude direction (x)	0.6165
Latitude direction (y)	1.1232
Altitude direction (z)	30.8952

Geotag variance: The difference between the image geotags and the optimized camera positions. Please note that these images geotag errors do not correspond to the accuracy on the observed 3D points.

### Ground control points

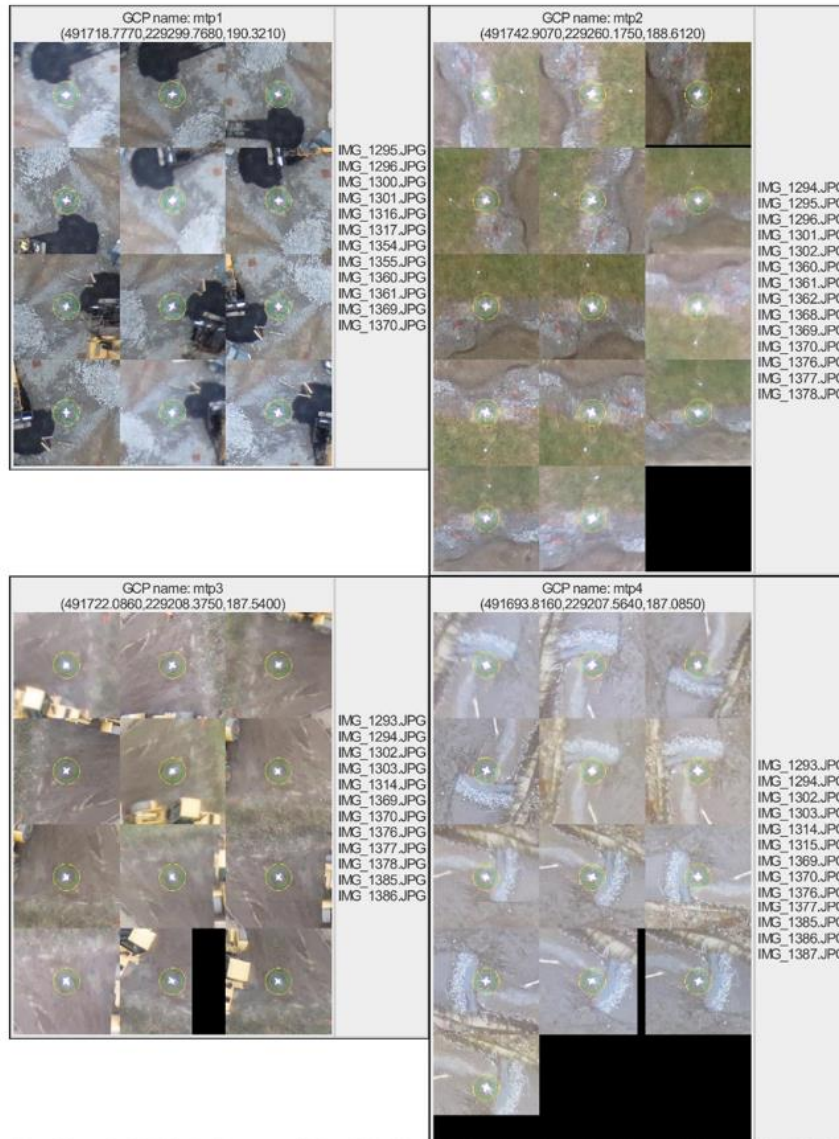


Figure 7: Images in which GCPs have been measured (yellow circle) and in which the 3D point have been projected (green circle). A green circle outside of the yellow circle indicates either an accuracy issue or a GCP issue.

# Appendix E: Shelburne sUAS Flight Quality Report

## Quality Report



See *Quality Report Help* for detailed explanations. Generated with version 3.0.3

### Summary

Project:	perpendicular_33cm
Processed:	2014-Jan-31 10:53:31
Camera name:	CanonIXUS127HS_4.3_4608x3456
Average Ground Sampling Distance (GSD):	3.14 cm
Area covered:	0.0233 km <sup>2</sup> / 2.3305 ha / 0.009 sq. mi.
Image coordinate system:	WGS84
Ground Control Point (GCP) coordinate system:	WGS84
Output coordinate system:	WGS84 / UTM zone 18N
Processing type:	full (scale 1) aerial
Time for Initial Processing (without report):	03m:33s

### Quality Check

<b>Images:</b>	median of 15641 keypoints per image	✓
<b>Dataset:</b>	37 out of 37 images calibrated (100%), all images enabled	✓
<b>Camera optimization quality:</b>	0.93% relative difference between initial and final focal length	✓
<b>Matching quality:</b>	median of 5421 matches per calibrated image	✓
<b>Georeferencing:</b>	no GCP	⚠

### Preview

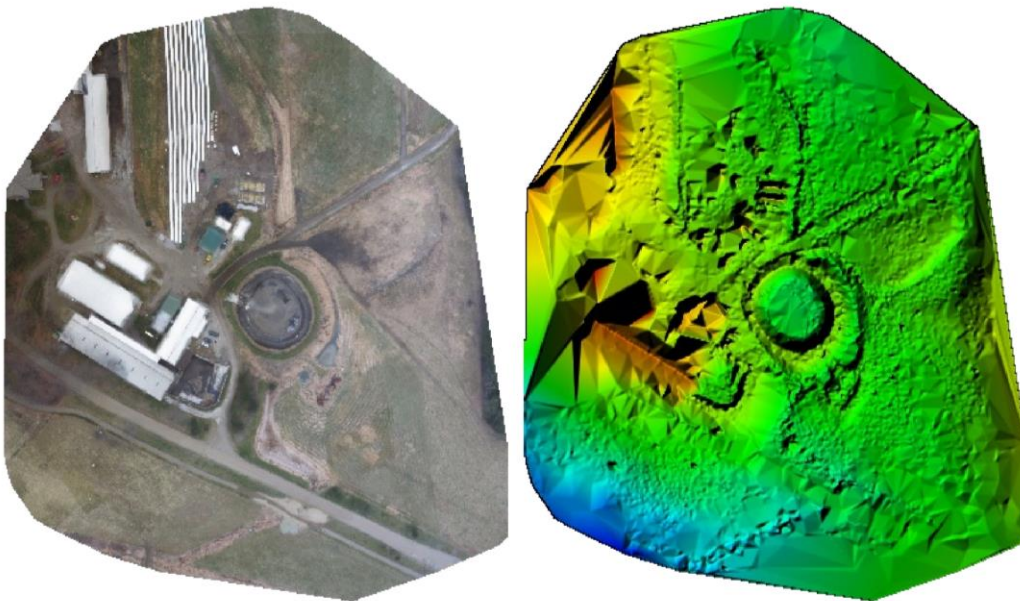


Figure 1: Ortho mosaic and the corresponding sparse digital surface model (DSM) before densification.

## Calibration details

Number of calibrated images:	37 out of 37
Number of geotagged images:	37 out of 37

### Geotag position

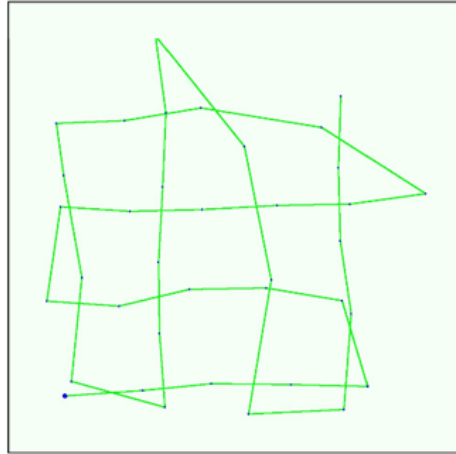


Figure 2: Top view of the geotags. The green line follows the geotags of the images in time starting from the large blue dot.

### Optimized camera position

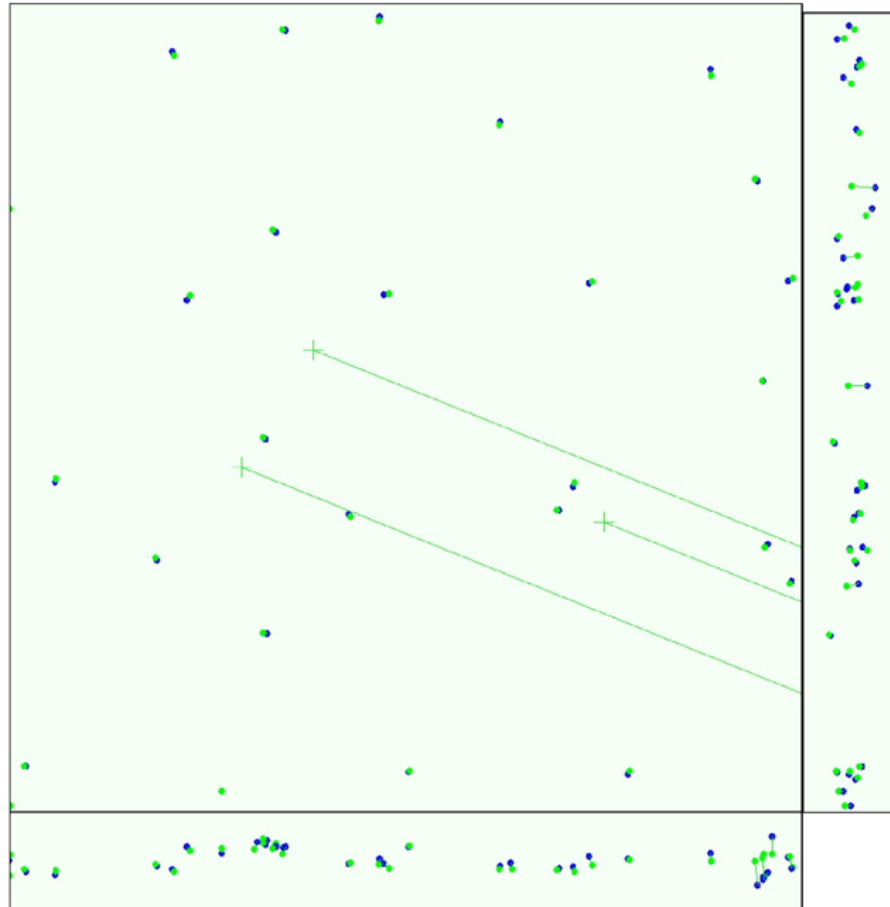


Figure 3: Offset between image geotags (blue dots) and optimized positions (green dots) as well as the offset between the GCPs positions (blue crosses) and their optimized positions (green crosses) in the top-view (XY plane), front-view (XZ plane) and side-view (YZ plane).

## Overlap

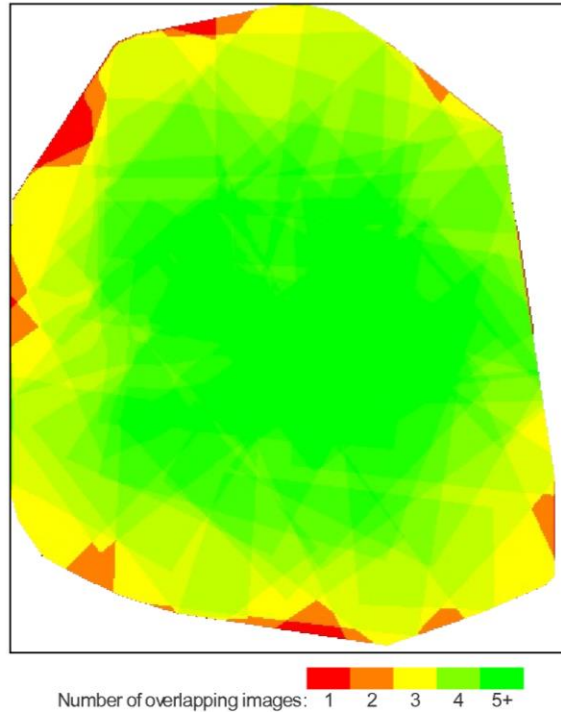


Figure 4: Overlapping score computed for each pixel of the orthomosaic. Red indicates areas where the overlap between the images is too low and could lead to poor results. For good quality results, the overlap should be over 5 images (green) for every pixel of the mosaic.

## Bundle Block Adjustment details

number total keypoint observations (automatic tie points) for bundle block adjustment	232755
number total 3D points for bundle block adjustment	86336
mean reprojection error	0.167237 [pixels]

Internal Camera Parameters ⓘ CanonIXUS127HS\_4.3\_4608x3456. Sensor dimensions: 6.17 [mm] x 4.63 [mm]

EXIF ID: CanonIXUS127HS\_4.3\_4608x3456

	Focal length	Principal point x	Principal point y	R1	R2	R3	T1	T2
initial values	3270.924 [pix] 4.380 [mm]	2303.999 [pix] 3.085 [mm]	1728.000 [pix] 2.314 [mm]	-0.049	0.059	-0.036	0.000	-0.003
optimized values	3301.530 [pix] 4.421 [mm]	2362.108 [pix] 3.163 [mm]	1858.396 [pix] 2.488 [mm]	-0.036	0.031	-0.011	0.008	0.005

## 2D Keypoints Table

	Number of 2D keypoints per image	Number of matched 2D keypoints per image
Median	15641	5421
Min	7240	935
Max	34872	16007
Mean	16110	6291

### 3D points from 2D keypoints matches

	Number of 3D points observed
In 2 images	59375
In 3 images	13608
In 4 images	5580
In 5 images	2939
In 6 images	1774
In 7 images	1142
In 8 images	812
In 9 images	506
In 10 images	296
In 11 images	169
In 12 images	102
In 13 images	28
In 14 images	4
In 15 images	1

### 2D Keypoints Graph

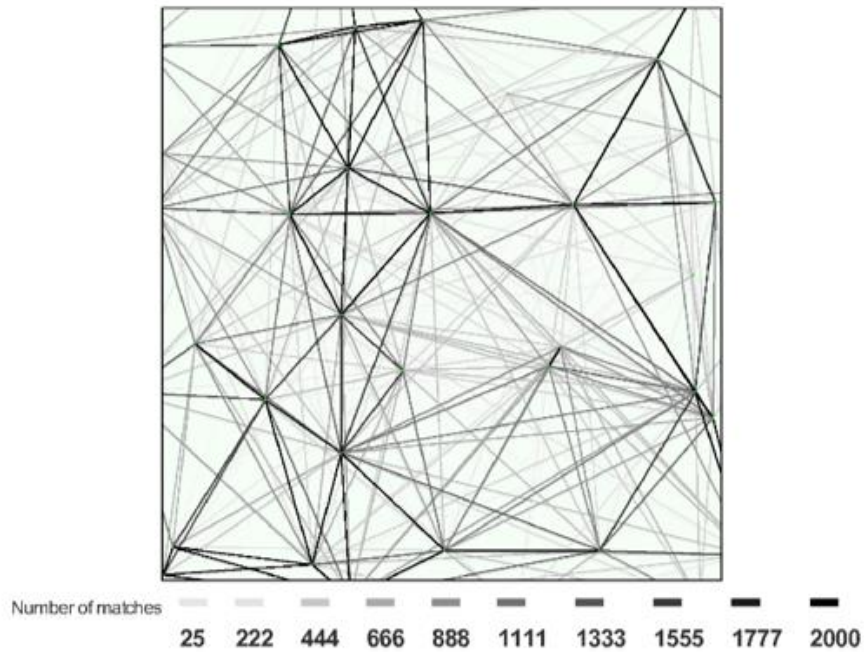


Figure 5: Top view of the geotags with a link between matching images. The darkness of the links indicates the number of matched 2D keypoints between the images. Bright links indicate low confidence and would require more overlap between the images or better quality images.

### Most visible 2D keypoints



Figure 6: Cropped area of 1 3D points arising from 15 2D keypoints. Each cropped area should represent the same 3D object.

## Geo-location and Ground Control Points

---

GCP name	tolerance [m]	error X[m]	error Y[m]	error Z [m]	projection error [pixel]	verified/ measured
User CP: mlp1	0.020				0.099	3 / 3
User CP: mlp2	0.020				0.120	5 / 5
User CP: mlp3	0.020				0.240	4 / 4

Localisation accuracy of the individual GCP, their mean error distance and the mean errors in the three coordinate directions. The last column counts the number of images where the GCP has been measured (clicked on the images) and on how many of them have been automatically verified. 0 out of 0 GCPs have been labeled as inaccurate (see Figure below).

### Geotag variance

Geotag localisation variance	sigma m
Longitude direction (x)	0.568
Latitude direction (y)	0.607
Altitude direction (z)	1.924

Geotag variance: The difference between the image geotags and the optimized camera positions. Please note that these images geotag errors do not correspond to the accuracy on the observed 3D points.

### Ground control points



## Appendix F: Standard Operating Guidelines

# Standard Operating Guidelines Sensefly eBee Unmanned Aerial System (UAS)

---



Updated 12/9/2013

Adam Zylka



## **Usage Permissions**

The Sensefly eBee Unmanned Aerial System (UAS) is currently under ownership of the US Department of Transportation (DOT) for use in the research project entitled “Rapid Exploitation of Commercial Remotely Sensed Imagery for Disaster Response & Recovery.” As such, it must first be used for flights associated with training, field calibrations, and testing related to this research. Permission to use the UAS must be obtained from the project’s Principal Investigator, Jarlath O’Neil-Dunne at the University of Vermont’s Spatial Analysis Lab (SAL). With prior approval from the US DOT Program Manager, Caesar Singh, it can be used for other projects that do not interfere with the primary research goals. Requests shall be submitted 30 days prior to its use on a project to Caesar Singh.

The work shall be prioritized in the following order:

- US DOT RITA (no user fees for use of UAS)
- Other Federal Agencies (no user fees for use of UAS)
- Other Non-Federal Agencies (user fees will be charged, but also need approval from US DOT RITA during project period)

## **User Fees**

To be determined.

## **Administrative Preparation**

After obtaining written permission to use the UAS from Jarlath O’Neil-Dunne and/or Caesar Singh, users will be required to obtain approval from Vermont Agency of Transportation (VTTrans) Aviation Program Administrator, Guy Rouelle, in accordance with the following steps:

- Guy Rouelle at the Vermont Agency of Transportation should be contacted at the onset of the project and provided with a project summary and scope of work.
- Flight will require a Mission Profile and during this initial conversation Mr. Rouelle will tell you exactly what information to include in the Mission Profile and how far in advance to submit it. Also, depending on where you want to fly and at what altitude, you may need a Certificate of Authorization (COA) for the flight. If your organization is not an Agency of the State, we recommend that you choose flight paths that are outside of restricted airspace and below 400ft AGL to avoid the COA requirement. Confirm with Mr. Rouelle as to whether or not your project will require a COA. If necessary, Guy Rouelle will contact FAA and Portland FSDO and/or obtain a Special Airworthiness Certificate (SAC).
- Send a Mission Profile to Guy Rouelle a minimum of 1 week prior to the scheduled flight. Generally, the Mission Profile should include the following information:
  - Location of departure and landing zones
  - Extent of flight area
  - Proposed flight path
  - Maximum in-flight altitude
  - Flight duration

Some additional items to consider when creating the Mission Profile:

- Restricted airspace: The general rule of thumb is that UAS should be flown 5 or more miles away from designated airports and Camp Johnson. However, different airports have different requirements and some additional restricted airspace exists within Vermont. Work with Guy Rouelle when selecting a flight location.
- Flight altitude: The UAS should be operated below 400ft (121m) AGL to avoid the need for FAA clearance.

## **Notifications**

The VTrans Secretary's office should be informed one week prior to any flights by contacting Steph Magnan ([Steph.Magnan@state.vt.us](mailto:Steph.Magnan@state.vt.us)). She will pass the information up the chain of command.

If the UAS flight is associated with a particular research project at UVM, the flight must be posted to the research project website at least one week before the flight.

In addition, it is highly recommended that the following entities should be contacted prior to the proposed flight:

- Local Police Department associated with the flight location
- State Police Department, if flying over or adjacent to state highways
- Property owners adjacent to flight location
- Local Municipality associated with flight location
- UVM Transportation Research Center Associate Director Glenn McRae

## **Equipment Acquisition**

The necessary equipment can be obtained from:

Spatial Analysis Laboratory  
Rubenstein School of Environment & Natural Resources  
220 George D. Aiken Center  
Burlington, VT 05405-0088  
Tel: (802) 656-3324

All users will be required to sign and date a sign-out sheet for the equipment and include contact information. In order to sign out the equipment, the user must present the following documentation:

- Permissions/approvals from Jarlath O'Neil-Dunne
- Permissions/approvals from Caesar Singh (if necessary).
- Documentation that Police, Property Owners, and Municipalities were contacted. If this was accomplished via telephone calls, you must provide documentation signed by your department head or Jarlath O'Neil-Dunne stating that this step was accomplished.

## Pre-flight Tasks

### 1. Charge batteries

- eBee battery packs (x3)
- Camera battery
- Handheld radios (x6)
- Laptop battery (x2)
- Check battery & operation of handheld wind meter

### 2. Ensure eMotion2 software and UAS firmware are up to date

1. Check for software updates: <http://www.sensefly.com/support/download.html>
2. Connect eBee battery
3. Connect eBee to PC via USB cable
4. Run 'Updater eBee' program (Start Menu->eMotion2-> Updater eBee)
5. Upon completion, unplug USB and disconnect battery
6. Connect battery to eBee & radio modem to PC
7. Open eMotion2 to ensure successful UAS/software connection

## Data Management

It is important that all data associated with UAS operations is organized in a consistent manner. General guidelines for spatial data management apply, including the absence of spaces or periods within file or folder names. Data should be organized as follows:

**Main folder:** Parent folder containing all data associated with a mission

*Convention:* [Day][Month][Year]\_[Project location or description]

*Example:* 07December2013\_SampleMission

### **Subfolders:**

**Flight Plans:** Contains all data associated with flight planning including:

- Flight plan XML
- Flight plan screenshot (JPG)
- Flight plan KML

This data should all be named using the following convention:

*Convention:* [Day][Month][Year]\_[Project location or description]

*Example:* 07December2013\_SampleMission

**Data Project:** Contains all data collected during mission and generated from processing. Folder and subfolders automatically created during creation of PostFlight Terra project and during data processing (refer to 'Data Processing' portion of document).

*Convention:* [Flight Number]

*Example:* Flight67

## *Standard Operating Guidelines: Sensefly eBee sUAS*

The following folders will be created automatically within this main directory during processing:

- **1\_initial**: contains flight quality report
- **2\_densification**: contains the densified and filtered point clouds
- **3\_dsm\_ortho**: contains the digital surface model, point cloud, and orthomosaic

### **Flight Planning**

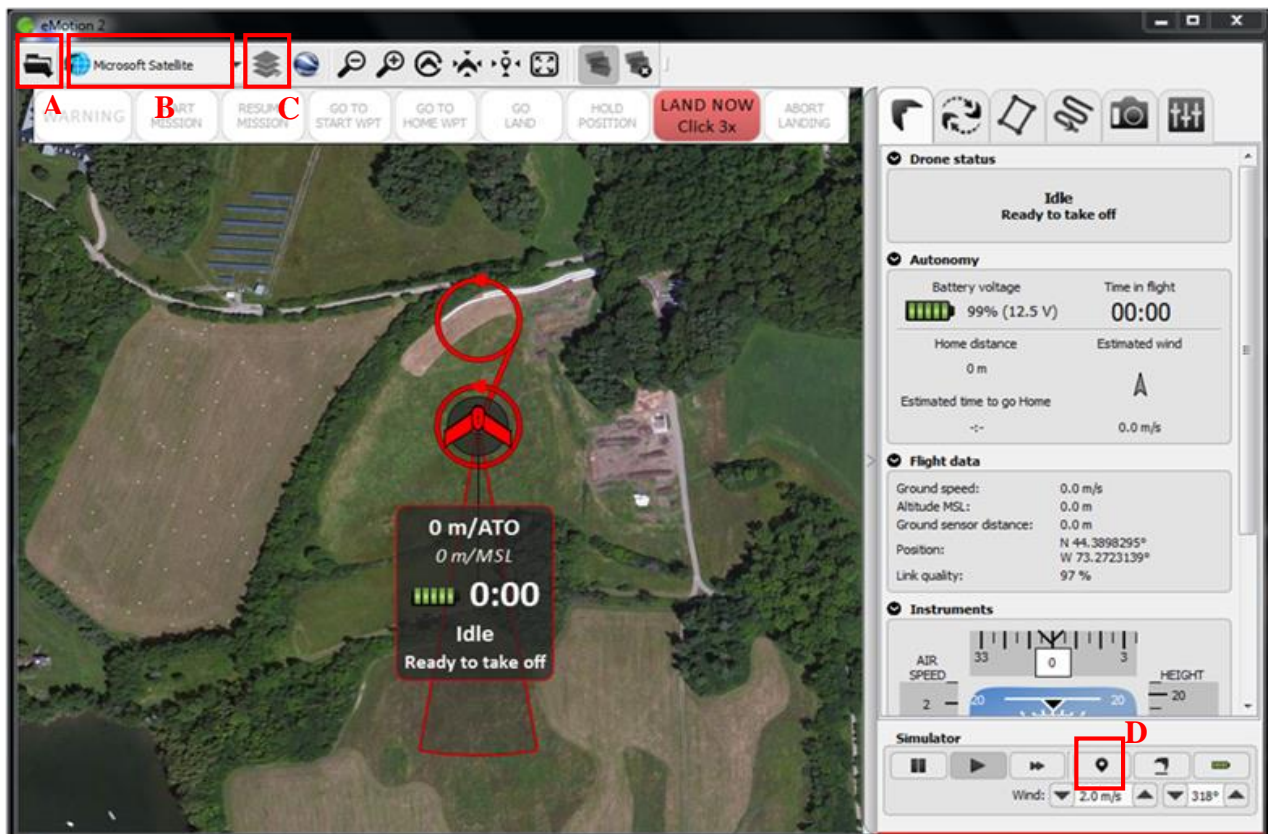
Creation of a flight plan should be accomplished at least 1 week prior to the date of proposed field operations to ensure timely notification and approval. Flight plans can be updated or created on site during operations, if necessary.

- 1. Launch eMotion 2 software**
- 2. Select “Simulator: eBee” option as shown and select ‘OK.’**

If a connection error warning is displayed, repeat this process (this is a known bug in the software).

### 3. Load base map and place proposed UAS start location

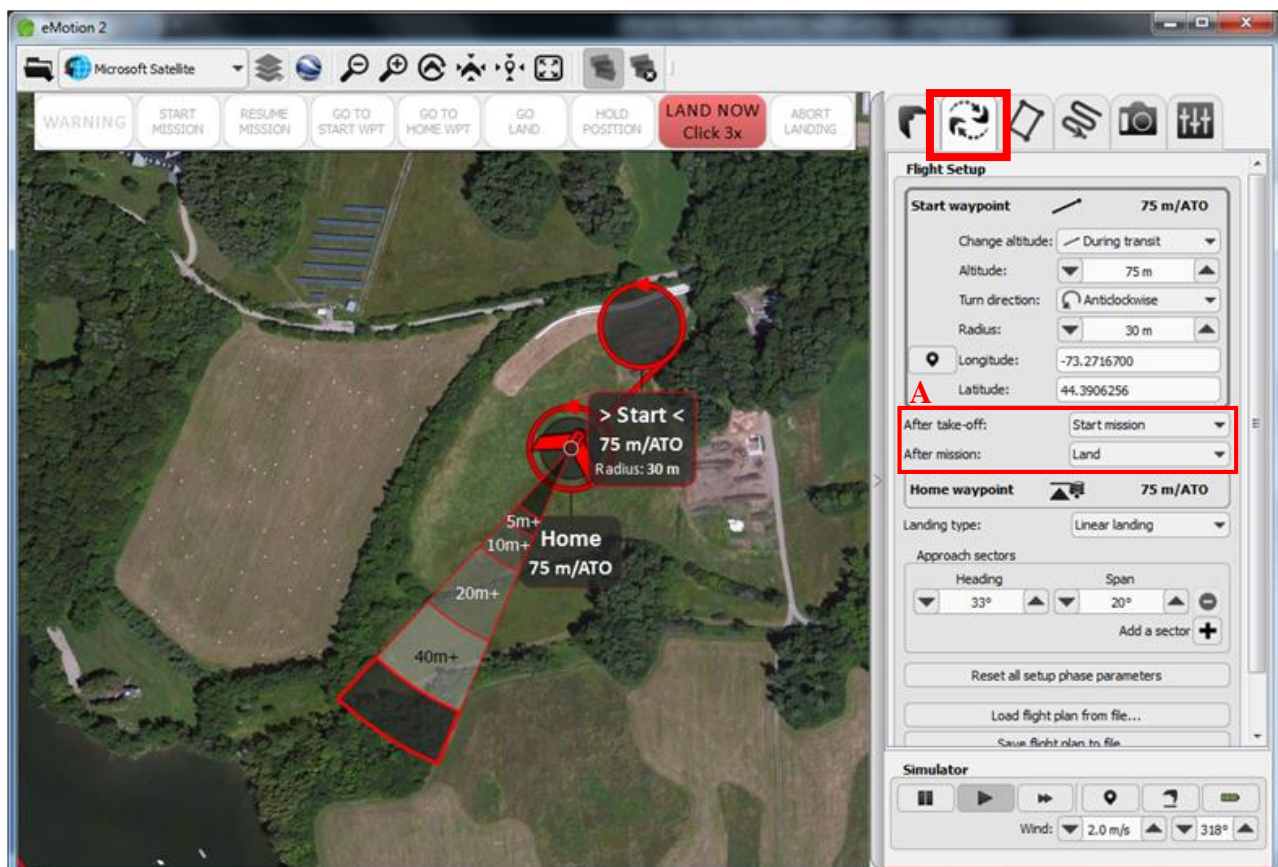
- Select a background map from the dropdown list (B) and pan to the area of interest for the flight.
- Select the marker icon in the lower right corner (D) of the drone status tab and use the crosshairs to select the proposed take-off location of the UAS.
- It is possible to import KML files as a custom basemap or for other planning purposes by selecting “Import KML (ctrl+j)” from the file dropdown menu (A) in the top left.
- The KML files available for viewing can be toggled on or off in the layers dropdown menu (C).



4. Place the estimated landing approach and home and start waypoints (Flight Setup tab)

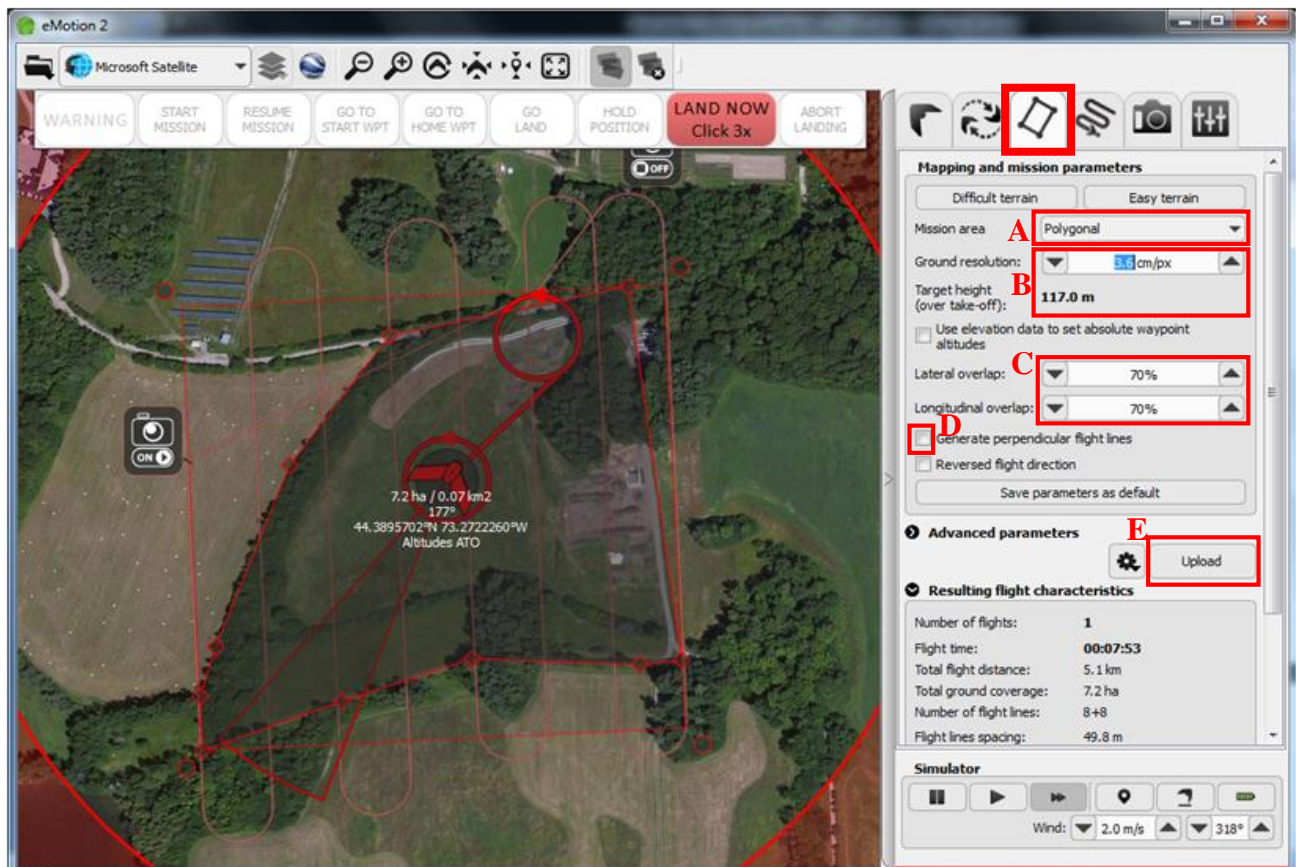
- **Home waypoint:** UAS landing location. Variable radius, 30m recommended.
- **Start waypoint:** UAS circles this location before initiating mission to gain altitude. Variable radius, 30m recommended.
- **Landing approach sector:** Zone of potential landing paths. Variable span and heading. Depending on field conditions, multiple approaches may be added. The eBee will select the best approach path based on wind conditions.
- By default, eBee will start mission after take-off and land immediately after mission completion. These actions can be adjusted with the dropdown menus (A).

These parameters can be adjusted by dragging with the mouse or by changing the associated values in the flight setup tab (highlighted). Generally, the start waypoint should be located up wind of the UAS launch location and the landing approach sector should be aligned so that the UAS is flying directly into the wind when landing. However, these locations are highly dependent on ground conditions and will require adjustment in the field.



## 5. Mission Planning

- Select mission area shape (A) and adjust rectangle or polygon to fit area of interest with mouse.
- Adjust desired ground resolution (B), ensuring the target height is below the 400ft (121m) FAA flight ceiling. Suggested values are between 2.5-3.5 cm/pixel.
- Specify lateral and longitudinal overlap (C). General guidelines are 65-70% lateral and 70% longitudinal for parallel flight lines, or 60-65% lateral and 70% longitudinal for perpendicular flight lines.
- Generate perpendicular flight lines when increased image overlap is desired by selecting the radio box (D). Note that this will approximately double the expected flight time.
- When complete, create the flight plan by selecting 'Upload' (E). The software will automatically create waypoints and flight lines according to the parameters specified.



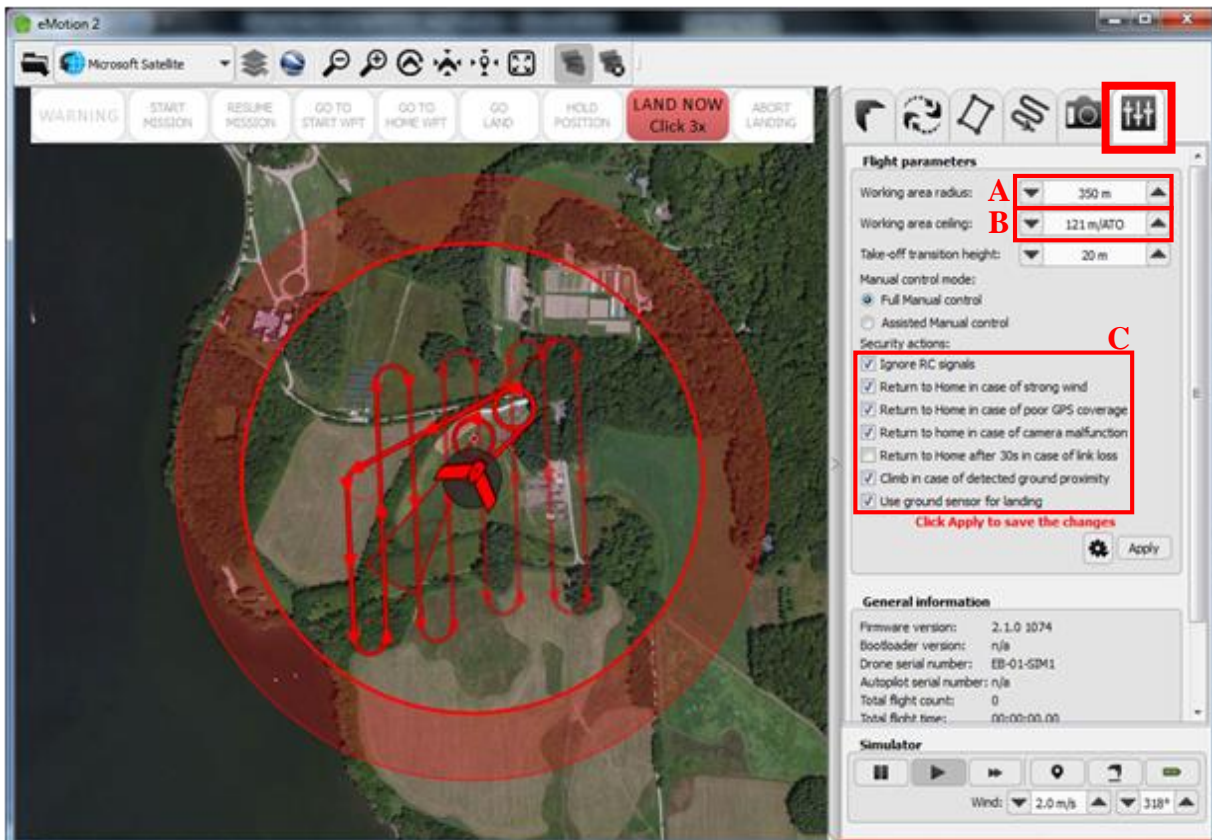


## 6. Mission Waypoints

If desired, a number of parameters can be adjusted for each of the mission waypoints either by selecting the waypoint on the map or by clicking the corresponding tab. In the majority of cases, no changes to waypoint attributes are necessary. This functionality is most useful for manual creation of flight plans, especially where a number of parallel flight lines mirroring a complex road corridor or stream are desired. Refer to the eBee manual for additional information.

## 7. Flight Parameters

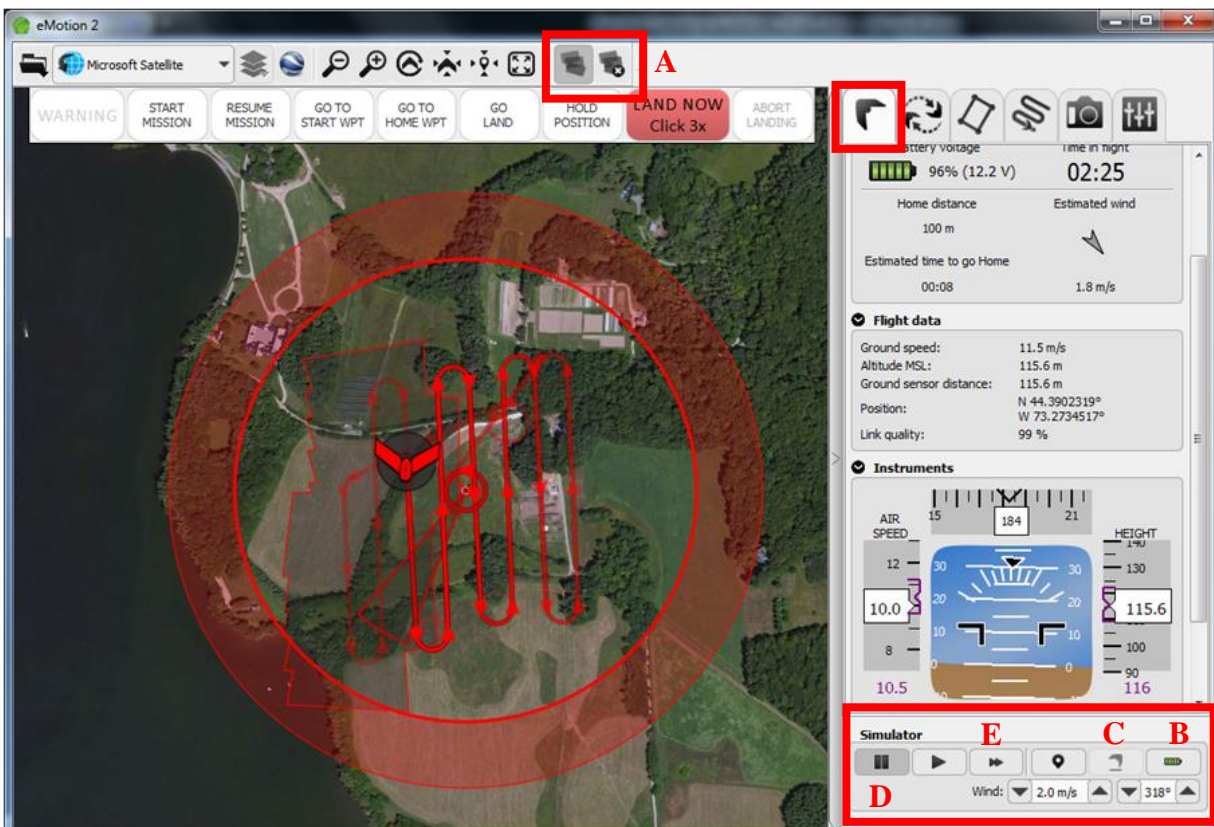
- Adjust working area radius (A) so that the flight path of the eBee is fully within the circle. This represents the maximum distance away from the launch location that the eBee will fly before returning to the Home waypoint.
- Adjust working area ceiling (B). This is the maximum elevation AGL that the eBee can achieve during flight. To comply with FAA regulations, the flight ceiling must be set to 400ft (121m) or less.
- Specify security actions (C) as shown.
- Click 'Apply' to save changes.



## 8. Simulate flight

It is recommended that the flight plan be simulated as a check of the proposed route and to ensure full photo coverage of the area of interest. Photography is simulated and coverage is displayed by an image footprint on the map. The footprint can be toggled on/off or reset (A).

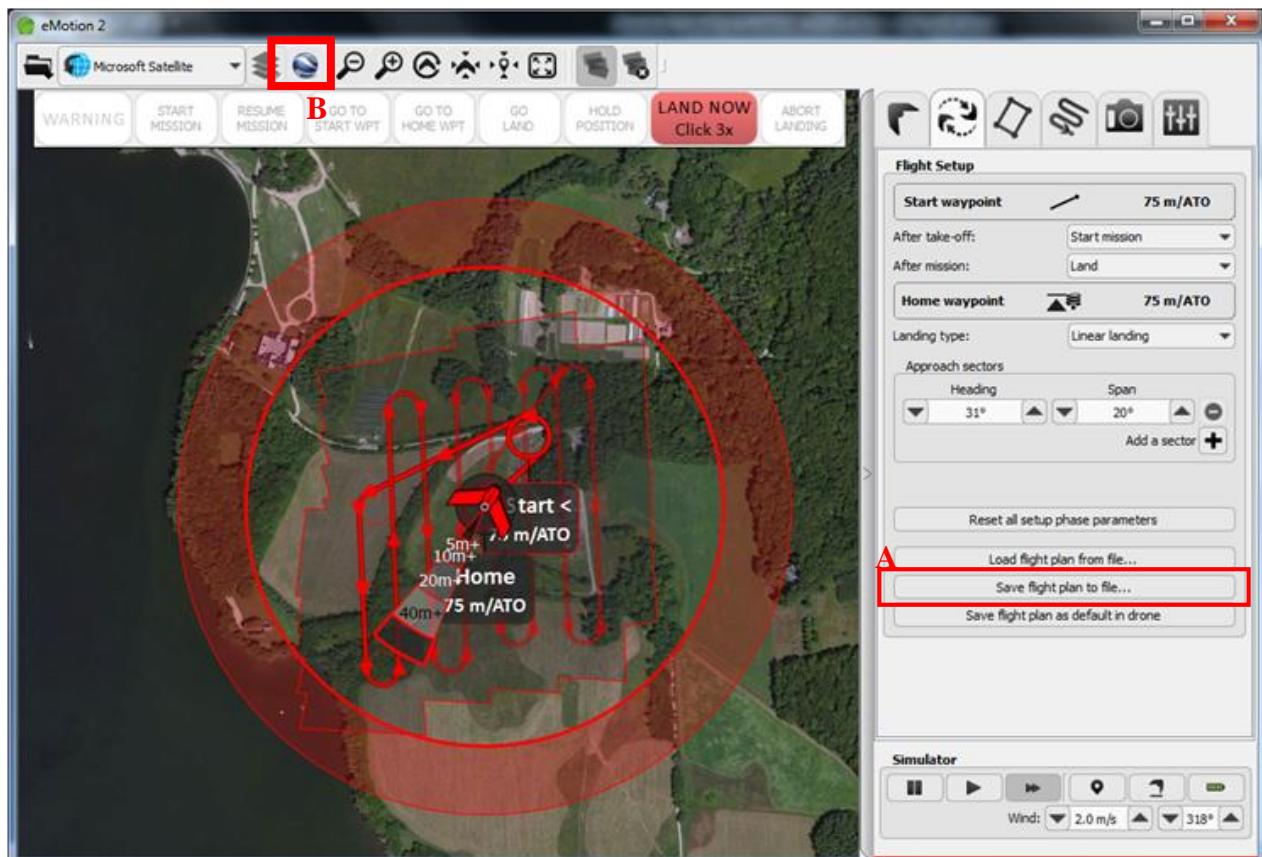
- Recharge simulated battery (B)
- Simulate take off (C)
- If desired, pause (D) or speed up (E) simulation
- Simulated wind speed and direction can be also be adjusted



## 9. Save finished flight plan

When flight plan has been finalized:

- Return to the Setup Phase tab (refer to Step 4 above)
- Select ‘Save flight plan to file...’ (A)
- Save output XML file according to location and naming convention previously discussed in ‘Data Management’ portion of document.
- Take a screenshot of flight plan and save according to location and naming convention previously discussed in ‘Data Management’ portion of document.
- Open flight plan in Google Earth (B) and save KML file according to location and naming convention previously discussed in ‘Data Management’ portion of document.



## 10. Cache background map data

At different levels of zoom, cache tiles of the desired background map data for the extent of the area to be flown by scrolling around the area until each imagery tile is displayed. This cache will be saved in the software even after the computer is shutdown. This is an important step in regards to in-flight monitoring and proper placement of the start and home waypoints when in the field. This step can be accomplished for multiple background map layers.

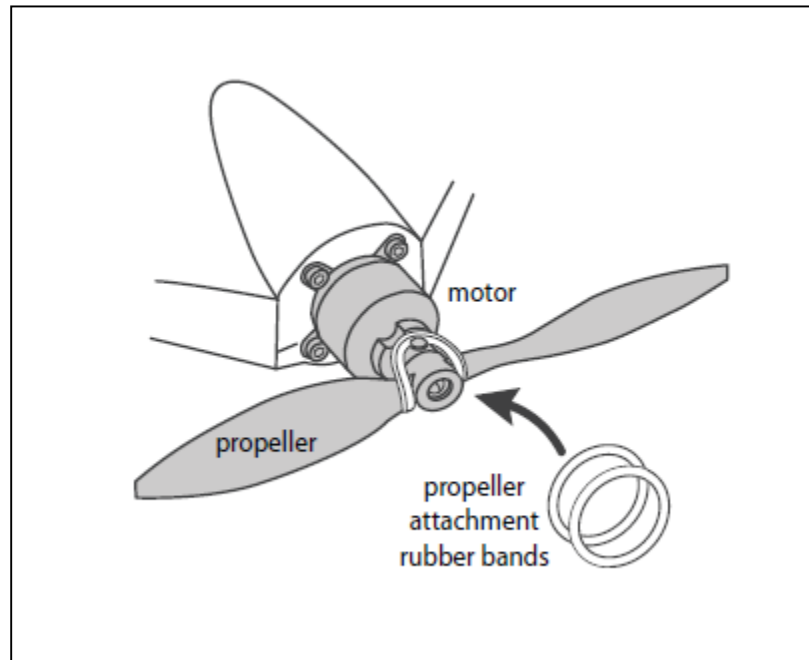
## Pre-flight Field Tasks

### 1. Perform general inspection of eBee

- Check the foam central body and wings for cracks or other damage.
- Verify that the pitot probe is properly attached to the airframe and that the holes in the probe are free of obstructions.
- Verify that the ground sensor is free of obstructions and that the sensor's lens is clean.
- Verify that the wing struts are not damaged.
- Verify that the power cables within the battery compartment are well insulated and not damaged.

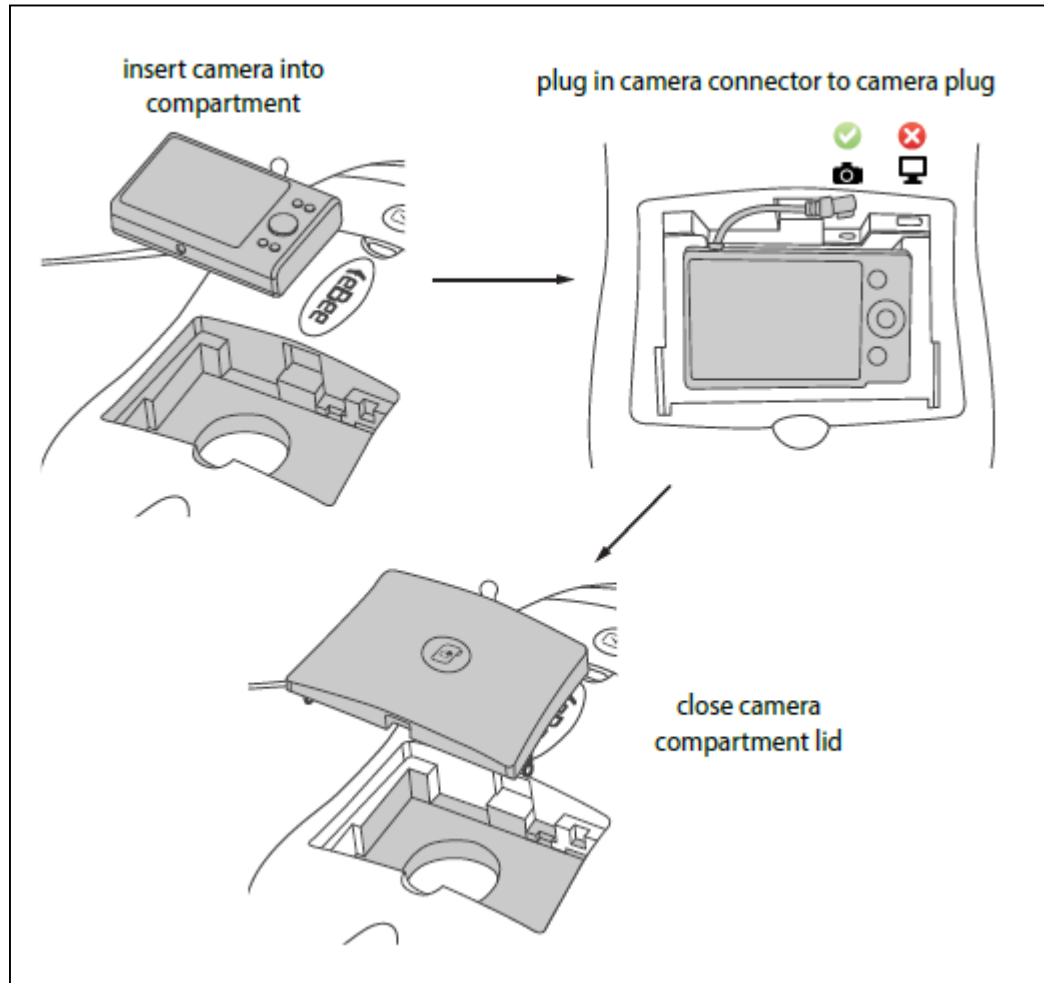
### 2. Install propeller

1. IMPORTANT: the metal ring of the propeller should be on the motor side.
2. Secure the propeller using two attachment rubber bands as illustrated below.
3. Ensure that the propeller is lying flat against the motor mount, and that the rubber bands do not show cracks or other signs of ageing.

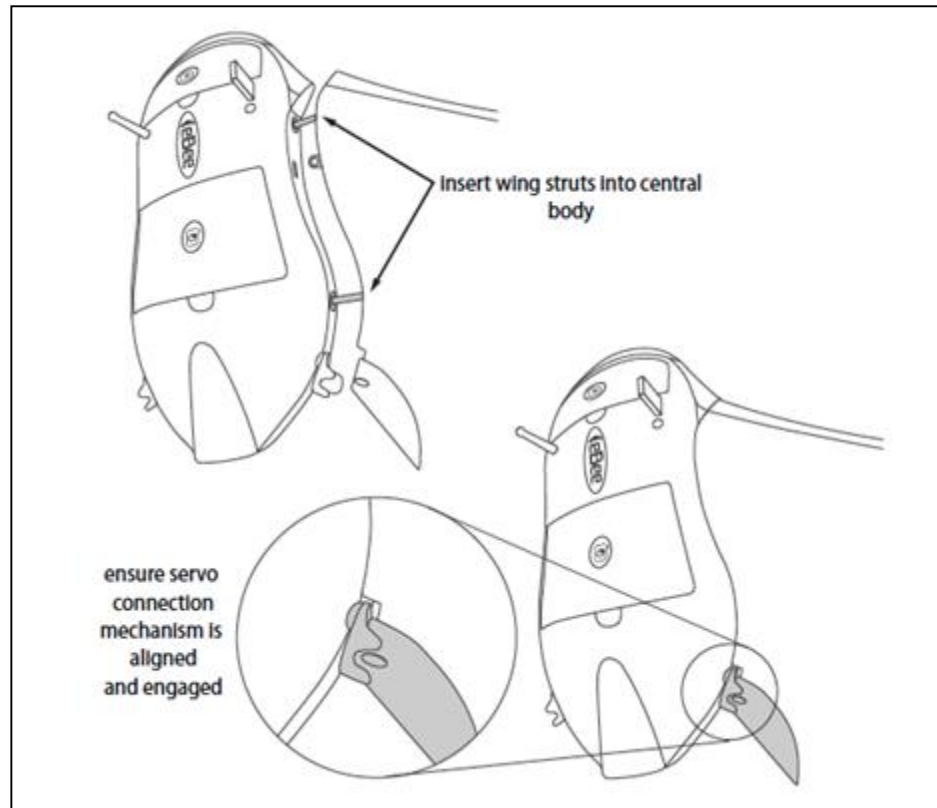


### 3. Connect camera

1. Insert battery & SD card
2. Remove foam cover for camera cavity
3. Connect camera to the eBee's internal port
4. DO NOT TURN ON CAMERA, it will be done automatically during flight
5. Replace foam cover



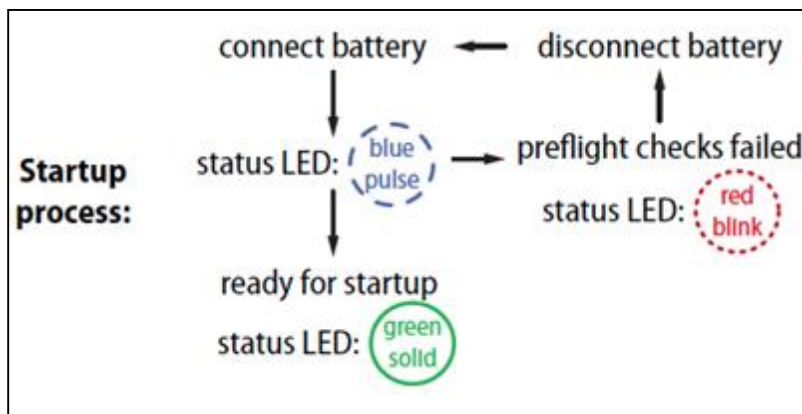
**4. Put the wings together with the body of the eBee and ensure that the servo connection mechanism is aligned and engaged (as show below)**



**5. Connect the battery (you must hear a “bip”) and close the battery compartment**

**6. Preflight tests**

1. Lay eBee flat on ground (no more than 10 degree incline), do not move during testing
2. eBee will self-check physical functions and acquire GPS signal (refer to step 8)
3. Status of preflight tests will proceed as shown:



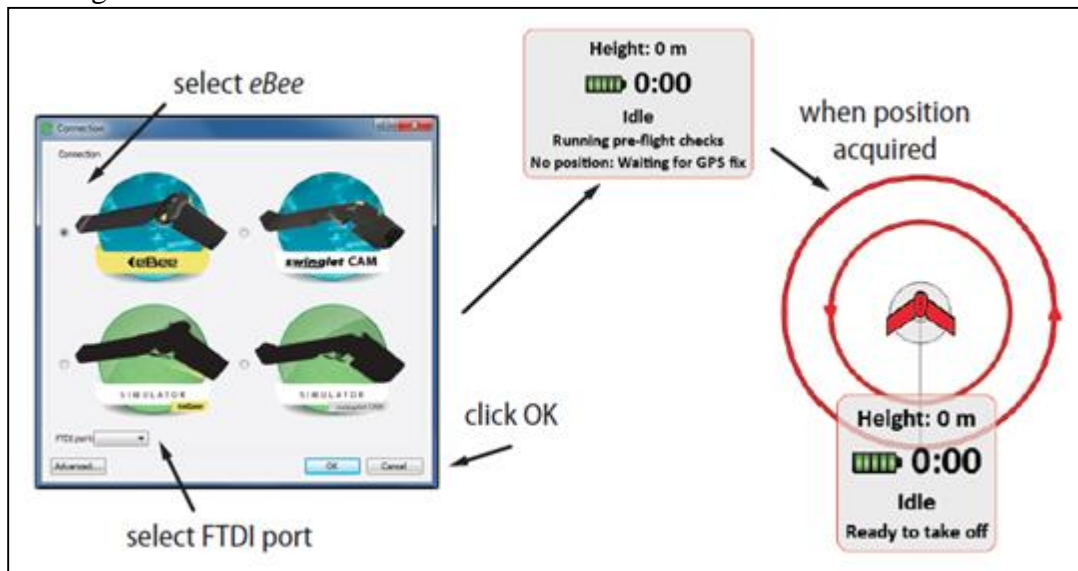
## 7. Connect senseFly radio modem to PC via USB

1. Flip power selector toggle switch to USB POWER
2. Ensure 3 red LEDs near antenna light up

## 8. Launch eMotion 2 (click on eBee, not on simulator) and select the FTDI port

## 9. GPS signal acquisition

Once the GPS position is acquired, an icon of the eBee will appear at its location on the map. The eBee's status in eMotion 2 will be displayed as 'Idle, Ready to takeoff' and the status LED will be solid green.



## 10. Load flight plan and upload to eBee

1. Select 'Load flight plan from file...' (Setup Phase tab)
2. Navigate to location of pre-made flight plan
3. Select and load flight plan into eMotion2

## 11. Adjust start waypoint and landing zone/approach (Setup Phase tab)

These locations should be adjusted according to topography and weather conditions. Generally, the start waypoint should be located up-wind from the launch location and the landing approach should be positioned facing the direction of the wind. It is also important to ensure that the landing approach path is clear of obstacles.

## 12. Check Flight Parameters

Navigate to Flight Parameters tab and ensure working area radius, flight ceiling, and security actions are correct. If changes are made, select 'Apply.'

## 13. IMPORTANT: Upload flight plan to eBee (Setup Phase tab)

Select 'Save flight plan as default in drone...' to upload flight plan to eBee. A green check mark will appear when successful.

**14. The eBee is now prepared for launch and to fly the mission. Follow protocol outlined in 'Flight Operations' section of this document.**

## **Flight Operations**

### **Flight crew:**

Prior to or upon arrival at the site, a chain of command should be established and the tasks that are expected of each crew member should be explicitly stated. Vital positions include:

- Flight commander (crew chief) – oversees flight crew and operations. Coordinates between operator and spotters.
- Flight operator – monitor flight from laptop computer. Makes all in-flight changes to flight path, including aborting mission or landing and putting UAS into holding pattern if landing zone is not clear
- Spotter(s) – maintain visual line of sight to UAS during flight and relay flight information to commander.

### **Safety:**

During all phases of flight operation, all crew members should wear high visibility vests. In areas near road corridors, construction sites, or locations where there may be any indication of potential safety issues, construction helmets are an additional safety requirement.

### **Communications:**

To ensure consistency in communications, guidelines for use of the handheld radios should be established prior to launch. Due to the requirement for visual line of sight at all times during a UAS flight, crew members may have to be positioned along the flight path and maintain communication by radio. These crew members should establish and verify their positions prior to take-off with the flight commander. A 'sterile cockpit,' where all communications should cease except those relevant to flight operation, should be maintained during take-off and landing procedures.

### **Launch:**

Hold eBee with two hands by front of wings. Shake eBee parallel to ground 3x to initiate propeller motion. Allow propeller to reach full speed (up to 5-10 secs). Gently propel eBee forward at a 10° angle from the ground in a lunging motion with extended arms. Release eBee to launch. Refer to eBee manual or trained crew member for further instruction.

### **Flight monitoring:**

Flights should be monitored using the eMotion 2 software. Any notifications of in-flight warnings will be displayed in the software interface. In addition, the eBee's mission or landing



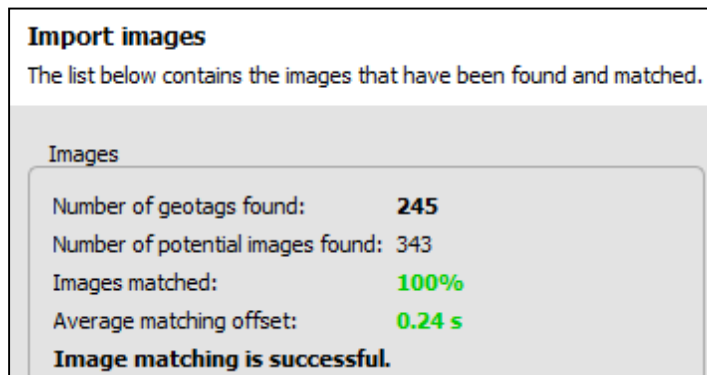
can be aborted if necessary or, if the landing zone is not clear, the UAS can be put into a circular holding pattern.

**Landing:**

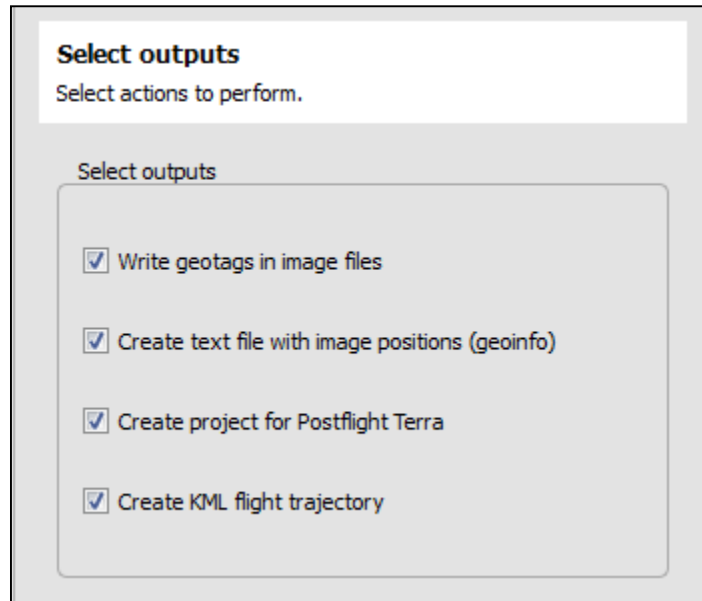
The landing zone should be cleared of any obstacles prior to initiation of the landing procedure. In most situations, it is recommended to program a linear landing pattern. Following the completion of a mission, the eBee will circle the designated home waypoint twice to determine wind conditions at the landing site. It will then automatically determine the best landing trajectory within the potential landing swath previously specified in the flight plan. During its descent towards the landing zone, the software will provide auditory notifications of the eBee’s altitude. Landing can be aborted at any time through the eMotion software. Following a successful landing, the software can be exited and the eBee’s battery removed.

**Data Processing**

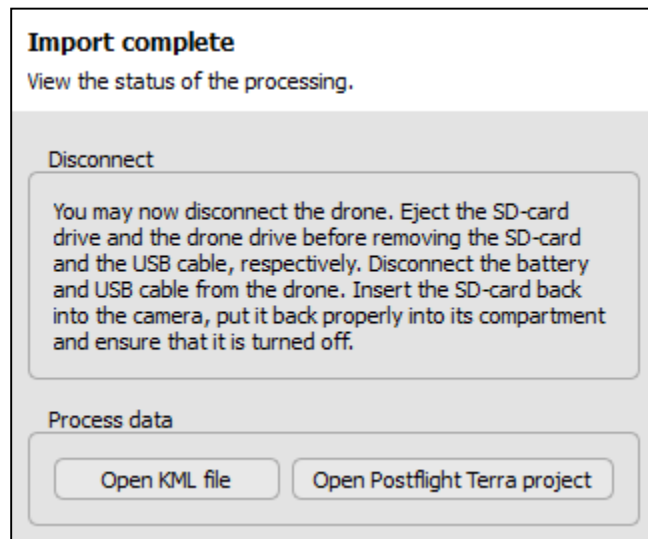
1. Connect eBee to computer via USB and connect battery. The UAS will display a white light.
2. Connect camera to computer via USB
3. Insert camera’s SD card into computer or copy contents of camera’s SD card to a temporary/scratch location on the computer
4. Open eMotion 2 software
5. Select ‘Flight Data Manager’ in connection window
  
6. Using the calendar and drop-down menu, select the flight of interest by date and time
7. Name the project with a descriptive name according to location and naming convention previously discussed in ‘Data Management’ portion of document.
8. Select ‘Next’
9. Browse to the camera’s SD card or temporary folder containing the copied images. The eBee flight log (.bbx file extension) will be imported automatically. Select ‘Next’
10. eMotion 2 will attempt to match images to the eBee flight plan. If image matching is successful, select ‘Next’ to copy images to project directory.




11. Select the following outputs and select 'Next' to create the project files



12. The following dialog will display when project file has been created. The flight plan and individual images can be viewed in Google Earth by selecting 'Open KML file.'



13. Select 'Open PostFlight Terra project.' It is safe to exit eMotion 2 when the project file opens.
14. If Ground Control Points (GCPs) were utilized in the mission, select the  toolbar icon to open the GCP Editor.
- A. Specify GCP coordinate system. All output files will be in same coordinate system.

Standard Operating Guidelines: Sensefly eBee sUAS

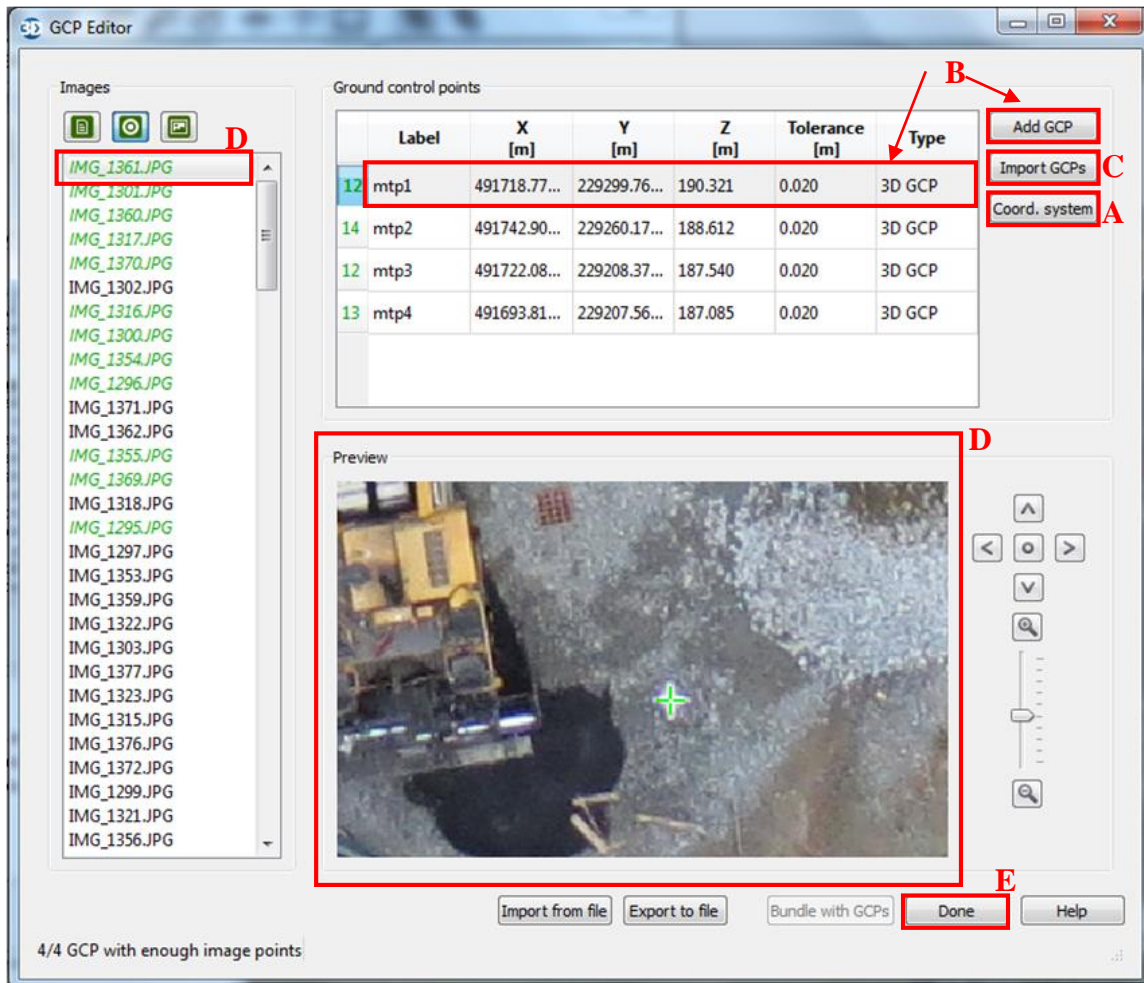
- B. Add new GCP and enter X,Y,Z data. The ‘Tolerance’ field will be automatically populated.
- C. Alternatively, GCPs can be batch imported by selecting ‘Import GCPs’ and navigating to a text file with the following structure:


[GCP#],[X coordinates],[Y coordinates],[Z coordinates]

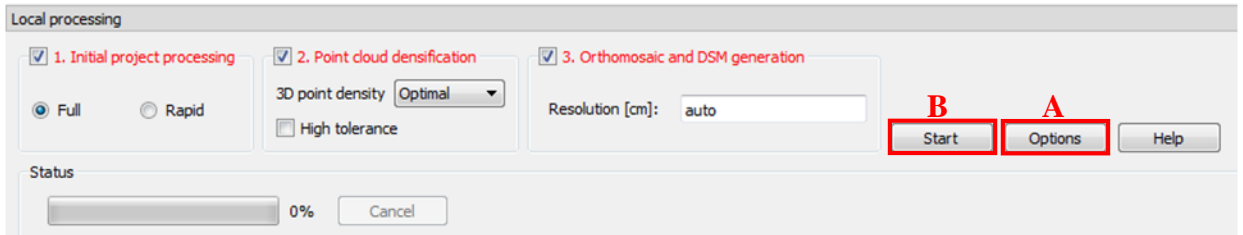
For example:


```
GCP0, 491718.777, 229299.768, 190.321
GCP1, 491742.907, 229260.175, 188.612
GCP2, 491722.086, 229208.375, 187.54
GCP3, 491693.816, 229207.564, 187.085
```

- D. For each GCP, use the cursor crosshairs to visually select the GCP in every image in which it appears. For projects with high overlap, each GCP may be represented in dozens of images.
- E. When complete, select ‘Done’ to save changes and exit the GCP editor



15. Select the  icon from the toolbar to open the ‘Local Processing’ menu.
- A. If necessary, adjust options for orthomosaic and point cloud. In most cases, this step is not needed.
- B. Initiate data processing. For most projects, the default options are recommended.



16. After processing has completed, the orthomosaic can be edited by selecting the  icon to access the ‘Scene editor’. Distance, area, and volume calculations can also be performed in this menu.

## Equipment Return

The following items must be performed when returning the equipment:

- Sign and date the sign-out sheet
- Note any changes to the equipment and notify Jarlath O’Neil-Dunne by email
- Plug in UAS batteries (x3), laptop batteries (x2), camera battery, and handheld radios to recharge